Final Report on a Multiple Discipline Geophysical Survey Blocks I, II, III, IV & V Northern Quebec

For

Waseco Resources Inc.
220 Bay Street – 3rd Floor
Toronto, Ontario
Canada, M5J 2W4

By

McPhar Geosurveys Ltd.
1256B Kerrisdale Blvd.
Newmarket, Ontario
Canada, L3Y 8Z9

January, 2006

McPhar 0506

TABLE OF CONTENTS

Page #

1. SUMMARY 10
2. INTRODUCTION 11
   - 2.1 Gravity Data Acquisition 12
   - 2.2 Magnetic and Radiometric Data Acquisition 13
3. SURVEY AREA 14
   - 3.1 Block I – Lac Bravo, Lac Crabe and Lac du Portage 16
   - 3.2 Block II – Lac Mistamisk 18
   - 3.3 Block III – Lac Drumlin 20
   - 3.4 Block IV – Lac Wawiyusi Anatwayach 22
   - 3.5 Block V – Lac Wawiyusi Anatwayach 24
4. SURVEY OPERATIONS 27
   - 4.1 Operations Base 27
   - 4.2 Survey Conditions 28
   - 4.3 Gravity Survey Technique / Methodology 29
     - 4.3.1 Establishment of GPS Base Stations 29
     - 4.3.2 Establishment of a Gravity Base Station Network 30
     - 4.3.3 Gravity Survey Logistics 32
     - 4.3.4 Navigation 32
     - 4.3.5 Gravity Survey Measurements 32
       - 4.3.5.1 Daily Loop Measurements 32
       - 4.3.5.2 Placing of the Gravity Meter on Station Locations 32
       - 4.3.5.3 Readings on Gravity Stations 33
     - 4.3.6 GPS Survey Measurements 33
     - 4.3.7 Gravity Survey Field Data Processing & Quality Control 34
     - 4.3.8 Gravity Survey Statistics and Project Diary 34
   - 4.4 Magnetic and Radiometric Survey Technique / Methodology 37
     - 4.4.1 Magnetic / GPS Base Station 38
     - 4.4.2 Magnetic and Radiometric Survey Logistics 38
     - 4.4.3 Navigation 39
     - 4.4.4 Magnetic and Radiometric Field Processing and Quality Control 39
     - 4.4.5 Magnetic and Radiometric Survey Statistics and Project Diary 39
5. HELICOPTER AND EQUIPMENT 41
   - 5.1 The Helicopter 41
   - 5.2 Gravity Survey Instrumentation Overview 42
     - 5.2.1 LaCoste & Romberg Gravity Meters 42
     - 5.2.2 TOPCON HyperLite GPS Systems 43
     - 5.2.3 Magellan eXplorist GPS Receivers 44
   - 5.3 Magnetic and Radiometric Survey Instrumentation Overview 44
     - 5.3.1 Airborne Magnetometer 45
     - 5.3.2 Gamma-ray Spectrometer System 45
     - 5.3.3 The Towed-Bird Airfoil and Tow-Cable 46
     - 5.3.4 The Base Station Magnetometer 46
     - 5.3.5 Altimeter 47
     - 5.3.6 The GPS Satellite Navigation System 47

5.3.7 Data Acquisition/Recording System 47
5.4 Field Computer Workstations 48
5.4.1 Spares 48
6. INSTRUMENT CHECKS AND CALIBRATIONS 49
6.1 Gravity Meter Tests and Calibrations 49
6.1.1 Instrument Calibrations 49
6.1.2 Scale Factor Test 49
6.2 Gravity Survey GPS Static Test 50
6.3 Airborne Magnetic System Tests and Calibrations 50
6.3.1 Magnetic Heading Effect 50
6.3.2 Lag Test 50
6.4 Airborne Gamma-ray Spectrometer System Tests and Calibrations 50
6.4.1 Test Line 50
6.4.2 Altitude Attenuation Coefficient 50
6.4.3 Cosmic Window Calibrations 50
6.4.4 Spectral Resolution Test 51
6.4.5 Daily Source Checks 51
6.5 Altimeter Calibration Checks 51
6.6 GPS Static Test 51
7. QC AND DATA PROCESSING 52
7.1 Gravity Survey Data Quality Control 54
7.1.1 Quality Control of Gravity Data Accuracy 54
7.1.2 Quality Control of Gravity Station Locations 55
7.1.3 Quality Control of GPS Data Quality and Bouguer Anomaly Accuracy 55
7.2 Preliminary Gravity Data Processing 56
7.2.1 Processing of the Gravity Data 56
7.2.1.1 Instrument Scale Factor 56
7.2.1.2 Tide Correction 57
7.2.1.3 Instrument Height Reduction 57
7.2.1.4 Drift Correction Calculation 58
7.2.1.5 Absolute Gravity Calculation 58
7.2.1.6 Processing of GPS Data 59
7.2.2 Integrated Processing of GPS and Gravity Data 59
7.2.2.1 Latitude Correction 59
7.2.2.2 Free Air Anomaly 60
7.2.2.3 Bouguer Anomaly Calculation 60
7.3 Final Gravity Data Processing 60
7.3.1 Calculation of Gravity Terrain Corrections 60
7.3.2 Processing of the Bouguer Anomaly and the Complete Bouguer Anomaly 62
7.3.3 WGS84 Ellipsoid Constants 63
7.3.4 Determination of the Bouguer Density 63
7.3.5 Gridding 64
7.3.6 Filter Derivatives 64
7.3.7 First Vertical Derivative 64
7.4 Airborne Survey Flight Path Compilation 65
7.5 Base Station Magnetic Data 65

7.6 Corrections to the Magnetic Data 65
7.6.1 Additional Corrections Applied to Profile Data 66
7.6.2 Gridding 66
7.6.3 Filter Derivatives 66
7.6.3.1 IGRF Removal 66
7.6.3.2 Reduction-to-the-Pole 67
7.6.3.3 Calculation of the First Vertical Derivative (1VD) 67
7.6.3.4 Calculation of the Second Vertical Derivative (2VD) 68
7.6.3.5 Calculation of the Total Horizontal Derivative (TOTHDRV) 68
7.6.3.6 Calculation of the Analytic Signal 68
7.7 Corrections to Radiometric Data 68
7.7.1 Background to Corrections and Processing 68
7.7.2 Processing Applied Using PRAGA 3 Radiometric Processing System 69
8. INTERPRETATION 71
8.1 Regional Geology 71
8.2 Regional Geophysical Setting 72
8.3 Regional Topographic Setting 75
8.4 Data Processing for Interpretation 77
8.4.1 Total Horizontal Derivative of the TMI and CBA 77
8.4.2 First Vertical Derivative (1VD) of the TMI and CBA 78
8.4.3 Second Vertical Derivative (2VD) of the TMI 78
8.4.4 Analytic Signal 79
8.4.5 Source Parameter Imaging 80
8.4.6 Euler Deconvolution Depth Estimates 80
8.4.7 Source Edge Detection 82
8.4.8 Radiometric Ratios and Ternary Mapping 82
8.5 Interpretation of Survey Blocks 83
8.5.1 Block I – Lac Bravo, Lac Crabe and Lac du Portage 83
8.5.1.1 Geology 83
8.5.1.2 Gravity 83
8.5.1.3 Magnetics 84
8.5.1.4 Radiometrics 85
8.5.1.5 Discussion of Results 85
8.5.1.6 Recommendations 86
8.5.2 Block II – Lac Mistamisk 87
8.5.2.1 Geology 87
8.5.2.2 Gravity 88
8.5.2.3 Magnetics 88
8.5.2.4 Radiometrics 88
8.5.2.5 Discussion of Results 88
8.5.2.6 Recommendations 90
8.5.3 Block III – Lac Drumlin 91
8.5.3.1 Geology 91
8.5.3.2 Gravity 92
8.5.3.3 Magnetics 92
8.5.3.4 Radiometrics 92

8.5.3.5 Discussion of Results 93
8.5.3.6 Recommendations 93
8.5.4 Block IV – Lac Wawiyusi Anatwayach 94
8.5.4.1 Geology 94
8.5.4.2 Gravity 94
8.5.4.3 Magnetics 94
8.5.4.4 Radiometrics 95
8.5.4.5 Discussion of Results 95
8.5.4.6 Recommendations 96
8.5.5 Block V - Lac Wawiyusi Anatwayach 96
8.5.5.1 Geology 96
8.5.5.2 Gravity 97
8.5.5.3 Magnetics 97
8.5.5.4 Radiometrics 97
8.5.5.5 Discussion of Results 98
8.5.5.6 Recommendations 98
8.6 Summary 98
9. DELIVERABLE PRODUCTS 102
9.1 Maps 102
9.2 Digital Data 103
9.3 Report 103

LIST of FIGURES

Figure 1: Location of Waseco Resources Inc. multiple parameter geophysical surveys, Northern Quebec indicating the survey block areas (red) and the Lac Pau Lodge (blue). 14
Figure 2: Location of Survey Areas. 15
Figure 3: Aerial view of the survey area topography – Block I. 16
Figure 4: Aerial view of the survey area topography – Block II. 18
Figure 5: Block I and Block II survey area with planned gravity stations and planned flight lines 19
Figure 6: Aerial view of the survey area topography – Block III. 20
Figure 7: Block III survey area with planned gravity stations and planned flight lines. 21
Figure 8: Aerial view of the survey area topography – Block IV. 22
Figure 9: Aerial view of the survey area topography – Block V. 24
Figure 10: Block IV survey area with planned gravity stations and planned flight lines. 26
Figure 11: Arial view of Lac Pau Lodge operation base 27
Figure 12: Field office in Lac Pau Lodge 27
Figure 13: Typical survey conditions for the gravity component of the project. 28
Figure 14: TOPCON HyperLite GPS receiver collecting data on GPS base station. 30
Figure 15: Gravity operator taking reading at gravity base station 900 at the Lac Pau Lodge. 31
Figure 16: LaCoste & Romberg Gravity meter and TOPCON GPS receiver in field use. 33
Figure 17: Helicopter R44 landing close to gravity station in Block I 36

Figure 18: Crew in front Helicopter R44 at Lac Pau Lodge operation base. 37
Figure 19: Air Saguenay float plane (left) and remote fuelling of the R44 on the lakeshore, Block IV (right). 38
Figure 20: Helicopter C-GLMO with magnetic sensor bird. 41
Figure 21: Helicopter Robinson R44 Raven taking-off from Lac Pau Lodge. 42
Figure 22: LaCoste & Romberg Model G Land Gravity Meter 43
Figure 23: TOPCON HyperLite GPS System 43
Figure 24: Magellan eXplorist GPS Receiver 44
Figure 25: Geometrics G-822A cesium magnetometer 45
Figure 26: Geometric G-822A cesium magnetometer mounted in the towed-bird airfoil. 46
Figure 27: Diagram of gravity meter calibration loops. 49
Figure 28: Data Processing Flow Chart – Gravity Survey 52
Figure 29: Data Processing Flow Chart – Airborne Magnetic and Radiometric Survey 53
Figure 30: Geological Survey of Canada (GSC) 2 km regional Bouguer gravity grid of the survey areas. 73
Figure 31. Geological Survey of Canada (GSC) 2 km Total Magnetic Intensity grid of the survey areas. 74
Figure 32: SRTM 90 Elevation DTM with screened 1:250 000 topographic data and Survey Block locations. 76

LIST of TABLES

Table 1: Waseco Resources Inc. Gravity Survey Area Description 11
Table 2: Waseco Resources Inc. Airborne Survey Area Description 12
Table 3: Waseco Resources Inc. - Block I – Lac Bravo, Lac Crabe and Lac du Portage Survey Area Description 17
Table 4: Waseco Resources Inc. - Block II – Lac Mistamisk Survey Area Description 19
Table 5: Waseco Resources Inc. - Block III – Lac Drumlin Survey Area Description 21
Table 6: Waseco Resources Inc. - Block IV – Lac Wawiyusi Anatwayach Survey Area Description 23
Table 7: Waseco Resources Inc. - Block V – Lac Wawiyusi Anatwayach Survey Area Description 25
Table 8: Distances between individual survey areas and operation base in kilometres 28
Table 9: GPS Base Station Details for WGS84 Ellipsoid 29
Table 10: Overview of the six Gravity Base Stations 31
Table 11: Gravity Project Diary 34
Table 12: Overview of Gravity Station Accessibility by Helicopter 35
Table 13: Projected Versus Actual Measured Gravity Stations 36
Table 14: Gravity Survey Field Personnel 36
Table 15: Airborne Magnetic and Radiometric Project Diary 40
Table 16: Airborne Magnetic and Radiometric Survey Field Personnel 40
Table 17: Land Gravity Meters used on the Waseco Project 43
Table 18: Dual Frequency Geodetic GPS Systems used on the Waseco Project 43
Table 19: Standard Gamma-ray Spectrometer Data Acquisition Windows 45

Table 20: Overview of Gravity Measurement Accuracies for Individual Blocks 54
Table 21: An Overview of the Quality of the Gravity Station Locations 55
Table 22: Earth Tide Calculation Location 57
Table 23: Bouguer Densities used for each survey block as derived from Nettleton profiles 64
Table 24: Pole reduction parameters by survey Block.....67
Table 25: Detail Area corner coordinates, Block II 90
Table 26: Potential Uranium enriched boulder responses, Block IV.....96
Table 27: Anomaly Summary Table 99
Table 28: Additional Claim Staking Summary Table.....101

APPENDICES

APPENDIX 1 **Statement of Qualifications**

APPENDIX 2 **System Tests and Reports**

Land Gravity

- Gravity / GPS Base Station 900 Form
- Gravity / GPS Base Station 901 Form
- Gravity / GPS Base Station 902 Form
- Gravity / GPS Base Station 903 Form
- Gravity / GPS Base Station 904 Form
- Gravity / GPS Base Station 905 Form
- List of Gravity Base Stations Loops
- Results of Gravity Base Stations Tie Survey
- List of Gravity Loops of Scale Factor Test
- Results of Scale Factor Test
- List of Helicopter Flights
- Gravity Field Logs
- Daily Operations Report
- List of Stations Surveyed out of 60 m Radius from Ideal Station Location
- Gravity Accuracy Report
- List of Skipped Stations

Magnetometer & Gamma Ray Spectrometer

- Lag Test
- Heading Correction Test
- Altimeter Test
- Cosmic Attenuation Coefficient Calibration
- Spectrometer Coefficient Calibration
- Flight Logs
- Daily Reports

APPENDIX 3 **Equipment Documentation**

- Robinson R 44 Helicopter
- LaCoste & Romberg Gravity Meter
- LaCoste & Romberg Set-up and Calibrations Instructions
- LaCoste & Romberg Scale Factors
- TOPCON HyperLite GPS System
- Magellan eXplorist Navigator
- OmniSTAR 3000 Real Time GPS System
- Geometrics G-822A Cesium Magnetometer
- Pico-Envirotec GRS-410 Multi-channel Gamma-Ray Spectrometer
- Field Data Processing Workstations
- Geosoft Montaj Processing Software

APPENDIX 4 **Personnel Resumes**

- Dallas Antill
- Tomas Grand
- Robert Hearst
- Juraj Vanik
- Juraj Kovacik
- Allan Tremblay

APPENDIX 5 **Principal Facts of Gravity & GPS Survey, Digital Data Specifications**

APPENDIX 6 **Page Size Maps**

For each area surveyed, the following map products have been prepared:

Gravity Maps

- Gravity Station Locations
- Digital Terrain Model (DTM)
- Free Air Anomaly
- Bouguer Anomaly, Bouguer Density = 2.45 gm/cc
- Bouguer Anomaly, Bouguer Density = 2.67 gm/cc
- Bouguer Anomaly, Bouguer Density = 2.80 gm/cc
- Calculated Terrain Correction (Bible Zones A to M)
- Complete Bouguer Anomaly, Bouguer Density = 2.45 gm/cc
- Calculated First Vertical Derivative (1VD) of the of the Complete Bouguer Anomaly, B.D. = 2.45 gm/cc
- Analytic Signal of the of the Complete Bouguer Anomaly, B.D. = 2.45 gm/cc
- Euler Deconvolution Depth Solution, S.I. = 0.0 of the Complete Bouguer Anomaly, Bouguer Density = 2.45 gm/cc
- Euler Deconvolution Depth Solution, S.I. = 1.0 of the Complete Bouguer Anomaly, Bouguer Density = 2.45 gm/cc

Magnetic & Radiometric Maps

- Flight Path with Planimetry
- Digital Terrain Model (DTM)
- Total Magnetic Intensity (TMI)
- Reduction to the Magnetic Pole of the TMI (RTP)
- Calculated Total Horizontal Derivative of the TMI - RTP
- Calculated First Vertical Derivative (1VD) of the TMI – RTP
- Calculated Second Vertical Derivative (2VD) of the TMI - RTP
- Calculated Analytic Signal of the TMI – RTP
- Keating Correlation Coefficient
- Source Parameter Imaging (SPI) Depth Estimates
- Magnetic Euler Deconvolution Depth Solution, S.I. = 1.0
- Magnetic Euler Deconvolution Depth Solution, S.I. = 2.0
- Source Edge Detection (SED)
- Radiometric Total Count (eTC)
- Radiometric Potassium (K)
- Radiometric Thorium (eTh)
- Radiometric Uranium (eU)
- Radiometric Uranium / Thorium Ratio (eU/eTh)
- Radiometric Uranium / Potassium Ratio (eU/K)
- Ternary Map

1. SUMMARY

A multiple discipline geophysical survey program with land and airborne survey components was completed on Waseco Resources Inc. land holdings in the Wabush Area of Northern Quebec over five (5) claim blocks: Block I – Bravo Lake, Crabe Lake and Portage Lake, Block II – Lac Mistamisk, Block III – Lac Drumlin, Block IV – Lac Wawiyusi Anatwayach, Block V – Wawiyusi Anatwayach, under contract to Waseco Resources Inc. signed April 2005. The program consisted of two major phases: a detailed land gravity / GPS survey; and a high resolution helicopter airborne magnetic and radiometric survey.

Data acquisition for the ground phase (land gravity / GPS Survey) was initiated on 22 June 2005 and completed on 8 July 2005. In all a total of 539 gravity stations, 38 repeat readings and 6 gravity/GPS base stations of data was collected, covering an area of 98 square kilometre. The gravity stations were surveyed on ground using Robinson R44 Raven helicopter for gravity crew and equipment transportation. The gravity stations were surveyed on rectangular grid at 500 m intervals and approximately oriented in north-south direction.

Data acquisition for the airborne phase (high-resolution airborne magnetic and radiometric survey) was initiated on 14 September 2005 and completed on 16 September 2005. In all a total of 1,104 line – kilometres of magnetic and radiometric data was acquired. The aircraft used for the towed bird magnetometer system was a Robinson R44 Raven. The spectrometer pack was mounted in the rear passenger compartment of the helicopter. Flight lines were oriented east-west with a line separation of 100 metres and tie lines were oriented north-south with a line separation of 1000 metres.

The multiple discipline geophysical surveys over Blocks I, II, III, IV and V have identified fifty-five (55) targets for additional study as a prelude to drill target selection. The anomalies are summarised as follows:

- 27 Uranium anomalies (25 High Priority; 2 Moderate Priority)
- 21 magnetic anomalies (17 High Priority, 1 Moderate Priority, 3 Low Priority)
- 7 Uranium boulder anomalies (All Low Priority)

The recommended follow-up studies are to incorporate all or some of the following methodologies:

- Geologic mapping including prospecting using a Geiger counter or hand held spectrometer and grab sampling,
- Heavy mineral sampling for kimberlite indicator minerals where appropriate,
- Geochemical sampling, including stream sediment and lake sediment sampling where appropriate for copper, gold and silver in addition to uranium,
- Till sampling in areas where glacial overburden coverage is a problem,
- Ground magnetometer surveying to confirm the location of the magnetic targets,
- Ground spectrometer surveying to be used to calibrate and confirm the airborne radiometric survey.
- Detailed surveying for conductive sulphide deposits at depth using either IP or TDEM where appropriate.

2. INTRODUCTION

A multiple discipline geophysical survey program with land and airborne survey components was completed on Waseco Resources Inc. , hereinafter referred to as "Waseco", by McPhar Geosurveys Ltd, hereinafter referred to as "McPhar", over five (5) claim blocks: Block I – Bravo Lake, Crabe Lake and Portage Lake, Block II – Lac Mistamisk, Block III – Lac Drumlin, Block IV – Lac Wawiyusi Anatwayach, Block V – Wawiyusi Anatwayach, in the Wabush Area of. Northern Quebec, under contract to Waseco Resources Inc. signed April 2005. The program consisted of two major phases: a detailed land gravity / GPS survey; and a high resolution helicopter airborne magnetic and radiometric survey.

The detailed land gravity / GPS survey was carried out during the period of 22 June 2005 to 8 July 2005. The detailed high-resolution helicopter-borne magnetic and radiometric survey was completed during the period of 14 September 2005 to 16 September 2005.

The purpose of the surveys was to acquire high-resolution geophysical data to map the gravity, magnetic and radiometric anomalies and geophysical characteristics of the geology and structure in an effort to provide an insight into geologic and geophysical settings conducive to economic uranium mineralization.

This report describes the surveys, the data processing and the data presentation.

Table 1: Waseco Resources Inc. Gravity Survey Area Description

AREA NAME	APPROX AREA KM^2	GRAVITY STATION SPACING	GRAVITY STATION TOTAL
Block I Bravo Lake, Crabe Lake and Portage Lake	44	500 m x 500 m	238
Block II Lac Mistamisk	15	500 m x 500 m	75
Block III Lac Drumlin	11	500 m x 500 m	63
Block IV Lac Wawiyusi Anatawayach	17	500 m x 500 m	100
Block V Lac Wawiyusi Anatawayach	11	500 m x 500 m	63
TOTALS	**98**		**539**

Table 2: Waseco Resources Inc. Airborne Survey Area Description

AREA NAME	APPROX AREA KM^2	LINE / TIE LINE SPACING	FLIGHT LINE-KM	TIE LINE-KM	TOTAL LINE-KM	PRIMARY FLIGHT LINE DIRECTION
Block I Bravo Lake, Crabe Lake and Portage Lake	44	100 m x 1000 m	449	40	489	90° / 270°
Block II Lac Mistamisk	15	100 m x 1000 m	153	17	170	90° / 270°
Block III Lac Drumlin	11	100 m x 1000 m	112	15	127	90° / 270°
Block IV Lac Wawiyusi Anatawayach	17	100 m x 1000 m	173	17	190	90° / 270°
Block V Lac Wawiyusi Anatawayach	11	100 m x 1000 m	117	11	128	90° / 270°
TOTALS	**98**		**1,004**	**100**	**1,104**	

2.1 Gravity Data Acquisition

A detailed land gravity / GPS survey was carried out during the period of 22 June 2005 to 8 July 2005 on behalf of Waseco by McPhar over the five (5) survey blocks in Northern Quebec, Canada.

The gravity data acquisition involved the use of four (4) precision differential GPS positioning systems and two (2) high sensitivity LaCoste & Romberg Model G gravity meters. The gravity stations were surveyed on ground supported by use of a Robinson R44 Raven helicopter for gravity crew and equipment transportation. Some areas were covered by thick forest with high trees or marshy ground. In these instances every effort was made to locate the gravity station such that a good view of a minimum of six (6) GPS satellites was obtained and that stable location was found for the gravity measurement. As a result of the thick bush and/or forest encountered, it was not possible to access as many stations by helicopter as had been expected prior to commencement of the survey; as a consequence, sixty-five percent (65 %) of the stations were accessed by helicopter. The remaining thirty-five percent (35%) of the gravity stations were accessed by foot.

The gravity stations were surveyed on rectangular grid at intervals of approximately 500 metres with a grid orientation of north-south.

Mobilization of the helicopter, equipment and personnel from Toronto and Ottawa to the operation base Lac Pau Lodge was completed over the period of 19 June to 22 June 2005. Production commenced on 23 June 2005. A fuel cache was established in the survey areas as required as the survey progressed.

Establishment of the GPS and local grid base gravity bases stations in the survey blocks was carried out progressively over the course of the survey. The gravity survey component was completed on 8 July 2005.

2.2 Magnetic and Radiometric Data Acquisition

A detailed high-resolution helicopter-borne magnetic and radiometric survey was completed during the period of 14 September 2005 to 16 September 2005 on behalf of Waseco by McPhar over five (5) survey blocks in Northern Quebec, Canada.

The data acquisition involved the use of precision differential GPS positioning, a high sensitivity magnetometer system towed beneath a helicopter and a multi-channel gamma-ray spectrometer with 16.8 litres "downward looking" NaI sensor. Ancillary equipment included a GPS navigation system with GPS base station, a radar altimeter, a base station magnetometer and a GPS base station.

Data was acquired along east-west oriented flight lines with a line separation of 100 metres and tie lines oriented north-south with a line separation of 1000 metres for each of the survey blocks. A mean terrain clearance of 25 metres for the magnetometer bird and 45 metres for the helicopter with spectrometer crystal pack onboard was maintained over all survey blocks.

Mobilization of the helicopter, equipment and personnel from Toronto and Ottawa to the operation base Lac Pau Lodge was completed over the period of 10 September to 13 September 2005. Production commenced on 14 September 2005. Fuel caches were established in survey areas I and II, area III and areas IV and V to optimize helicopter usage. The airborne survey component was completed on 16 September 2005.

3. SURVEY AREA

The survey consisted of five blocks identified by Waseco as:

- Block I – Lac Bravo, Lac Crabe and Lac du Portage
- Block II – Lac Mistamisk
- Block III – Lac Drumlin
- Block IV – Lac Wawiyusi Anatwayach
- Block V – Lac Wawiyusi Anatwayach

All blocks are located to the north and east of Lac Pau Lodge in the Northern Quebec, Canada. The primary objective of the surveys was to acquire gravimetric, magnetic and radiometric data in support of uranium exploration.

Figure 1: Location of Waseco Resources Inc. multiple parameter geophysical surveys, Northern Quebec indicating the survey block areas (red) and the Lac Pau Lodge (blue).

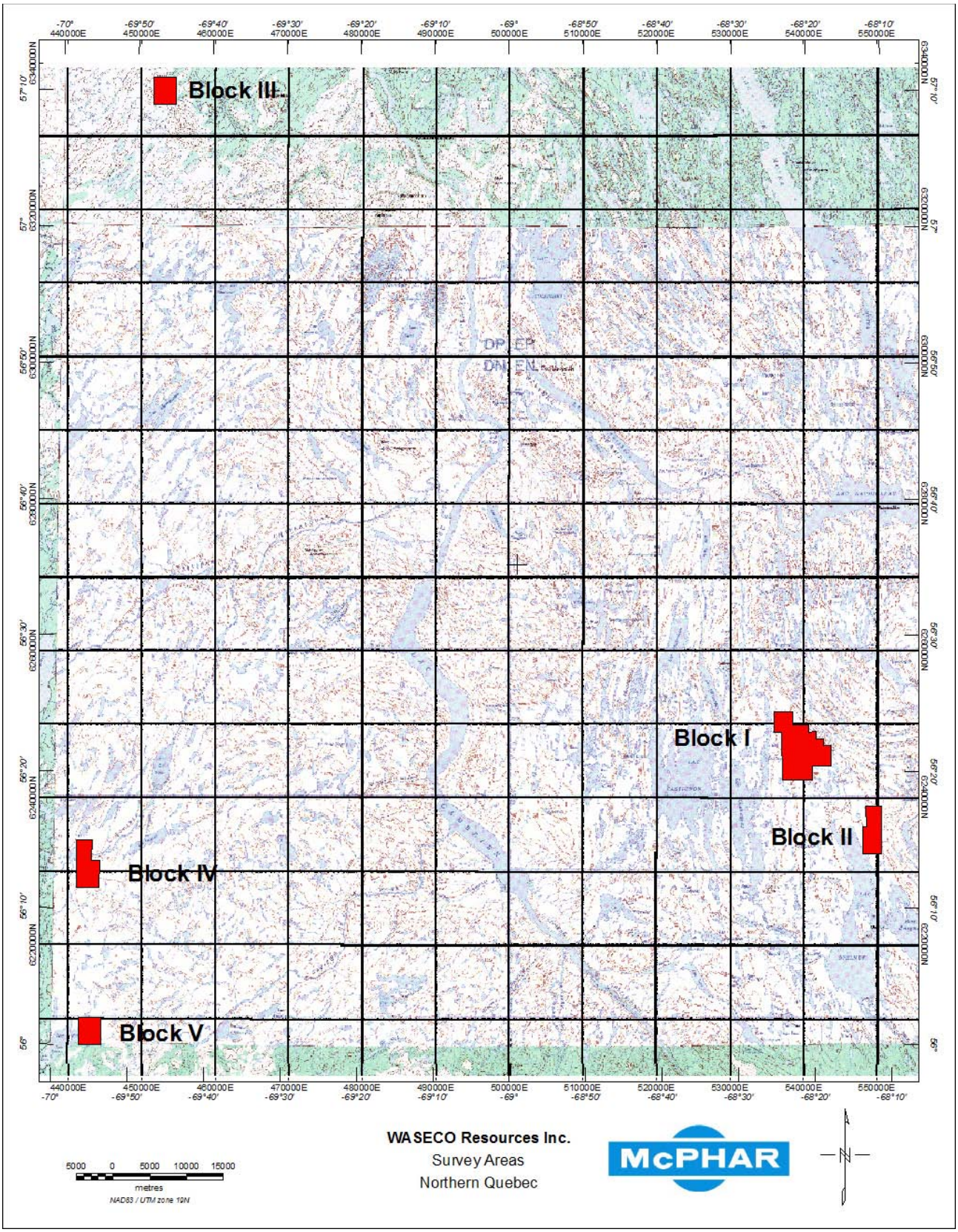

Figure 2: Location of Survey Areas.

3.1 Block I – Lac Bravo, Lac Crabe and Lac du Portage

Block I is located 190 km to the north-east of Lac Pau Lodge and between lakes Lac du Mortage and Lac Esker. The survey topographic relief is low and relatively flat. The block is dotted with numerous small lakes, ponds, rivers and marshy areas.

Weather conditions during the survey were typically cold (9°C) and partly cloudy with occasional showers. During the magnetic and radiometric survey, conditions were cold (0°C) and clear.

Figure 3: Aerial view of the survey area topography – Block I.

The survey block corner coordinates were provided by Waseco in NAD83 zone 19N UTM easting and northing. The following tables contain the survey block corner coordinates in NAD83.

Table 3: Waseco Resources Inc. - Block I – Lac Bravo, Lac Crabe and Lac du Portage Survey Area Description

Lac Bravo, Lac Crabe and Lac du Portage Block I		
Corner	UTM Easting	UTM Northing
1	537144	6242430
2	537087	6248923
3	536058	6248914
4	536035	6251647
5	538606	6251689
6	538623	6249864
7	540681	6249883
8	540690	6248956
9	541719	6248966
10	541728	6248038
11	542757	6248049
12	542767	6247121
13	543796	6247131
14	543825	6244349
15	541249	6244323
16	541267	6242468

Coverage Type (%)			
Boreal Forest	Tundra	Marshland	Outcrop
60	20	10	10

The gravity stations were surveyed on rectangular grid at 500 m intervals.

The magnetic and radiometric surveys were surveyed along east-west flight lines with a line separation of 100 metres. Tie lines were flown north-south with a line separation of 1000 metres.

The Block I Survey Area covered approximately 44 km².

3.2 Block II – Lac Mistamisk

Block II is located 190 km to the north-east of Lac Pau Lodge and to the east of Lac du Prospecteurs. The survey area is of low relief, dotted by small lakes, ponds, rivers and marshy areas.

Weather conditions during the survey were typically warm (20°C) and partly cloudy. During the magnetic and radiometric survey, conditions were cold (0°C) and clear.

Figure 4: Aerial view of the survey area topography – Block II.

The survey block corner coordinates were provided by Waseco in NAD83 zone 19N UTM easting and northing. The following tables contain the survey block corner coordinates in NAD83.

Table 4: Waseco Resources Inc. - Block II – Lac Mistamisk Survey Area Description

Lac Mistamisk Block E		
Corner	UTM Easting	UTM Northing
1	548082	6232301
2	548040	6236046
3	548556	6236052
4	548524	6238834
5	550588	6238858
6	550665	6232336

Coverage Type (%)			
Boreal Forest	Tundra	Marshland	Outcrop
33	26	11	30

The gravity stations were surveyed on rectangular grid at 500 m intervals.

The magnetic and radiometric surveys were surveyed along east-west flight lines with a line separation of 100 metres. Tie lines were flown north-south with a line separation of 1000 metres.

The Block II Survey Area covered an area of approximately 15 km².

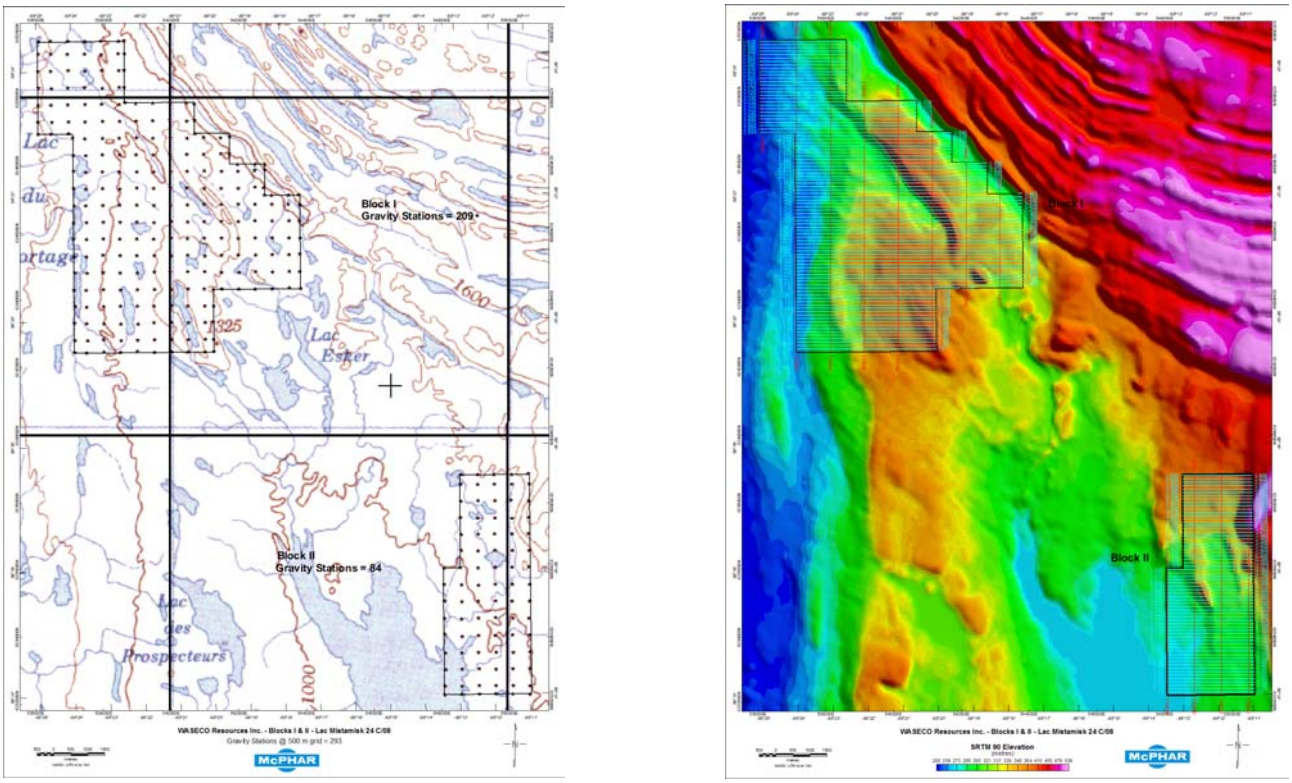

Figure 5: Block I and Block II survey area with planned gravity stations and planned flight lines

3.3 Block III – Lac Drumlin

Block III is located 260 km to the north of Lac Pau Lodge close to the Forbes River.

The survey area exhibits low topographic relief, gently downward sloping to the north-east. Within the survey area, the terrain rises from approximately 300 metres in north-east approximately 500 metres in the south-western part of the area. Weather conditions during the gravity survey were typically cold (10°C) and partly cloudy with occasional showers. During the magnetic and radiometric survey, conditions were cold (0°C) and clear.

Figure 6: Aerial view of the survey area topography – Block III.

The survey block corner coordinates were provided by Waseco in NAD83 zone 19N UTM easting and northing. The following tables contain the survey block corner coordinates in NAD83.

Table 5: Waseco Resources Inc. - Block III – Lac Drumlin Survey Area Description

Lac Drumlin NTS 24/F04 Block III		
Corner	UTM Easting	UTM Northing
1	451676	6338096
2	454699	6338062
3	454658	6334351
4	451633	6334385

Coverage Type (%)			
Boreal Forest	Tundra	Marshland	Outcrop
0	5	5	90

The gravity stations were surveyed on rectangular grid at 500 m intervals.

The magnetic and radiometric surveys were surveyed along east-west flight lines with a line separation of 100 metres. Tie lines were flown north-south with a line separation of 1000 metres.

The Block III Survey Area covered a total of approximately 17 km².

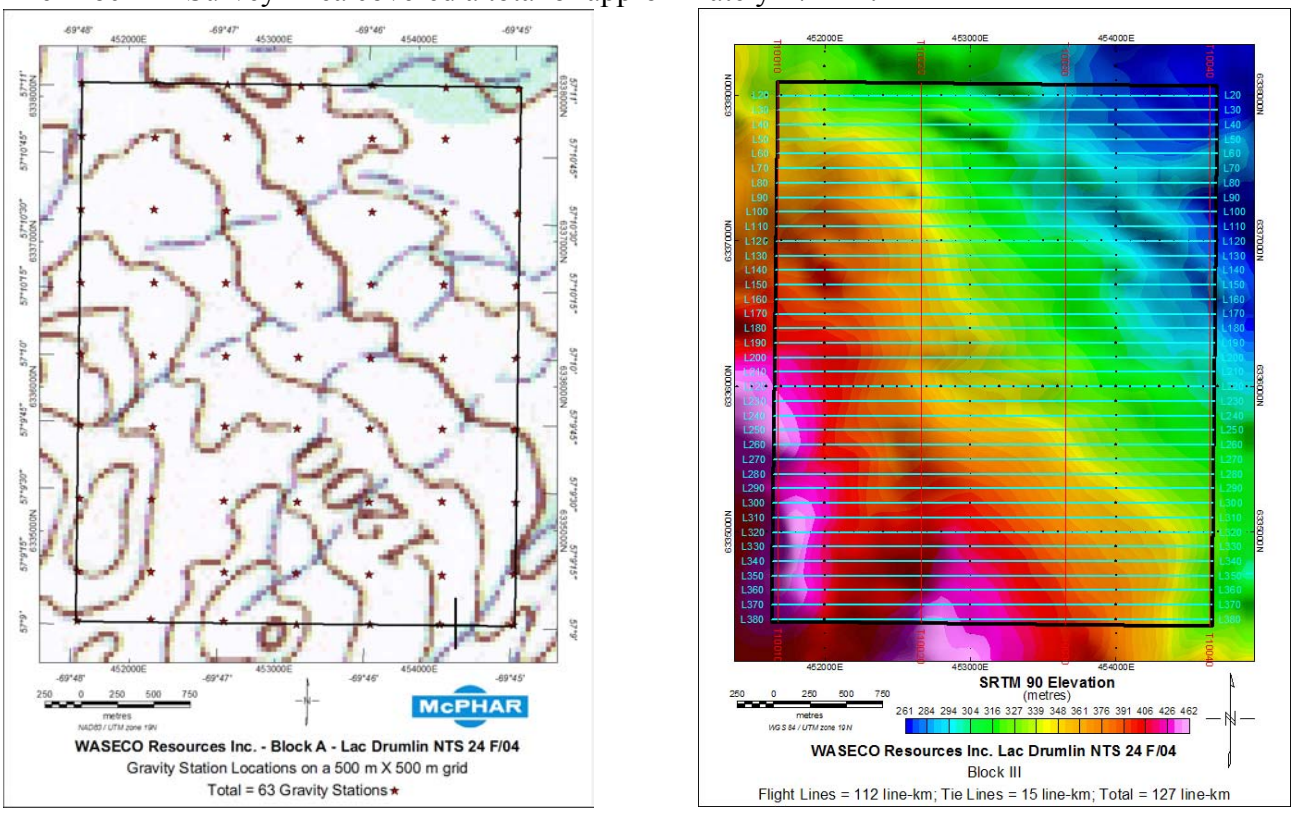

Figure 7: Block III survey area with planned gravity stations and planned flight lines.

3.4 Block IV – Lac Wawiyusi Anatwayach

Block IV is located 150 km to the north of Lac Pau Lodge and to the west of Lac Gerzine.

The survey area is of low, flat relief with a topographic ridge running from the southwest to the northeast.

Weather conditions during the survey were typically cold (10°C) and partly cloudy with occasional showers. During the magnetic and radiometric survey, conditions were cold (0°C) and clear.

Figure 8: Aerial view of the survey area topography – Block IV.

The survey block corner coordinates were provided by Waseco in NAD83 zone 19N UTM easting and northing. The following tables contain the survey block corner coordinates in NAD83.

Table 6: Waseco Resources Inc. - Block IV – Lac Wawiyusi Anatwayach Survey Area Description

Lac Wawiyusi Antawayach Block IV		
Corner	UTM Easting	UTM Northing
1	441080	6227834
2	441169	6234327
3	443235	6234299
4	443198	6231516
5	444231	6231502
6	444182	6227793

Coverage Type (%)			
Boreal Forest	Tundra	Marshland	Outcrop
25	40	15	20

The gravity stations were surveyed on rectangular grid at 500 m intervals of lines approximately oriented in north-south direction.

The magnetic and radiometric surveys were surveyed along east-west flight lines with a line separation of 100 metres. Tie lines were flown north-south with a line separation of 1000 metres.

The Block IV Survey Area covered a total of approximately 11 km².

3.5 ***Block V – Lac Wawiyusi Anatwayach***

Block V is located 130 km to the north of Lac Pau Lodge and on the north-east shore of Lac Pons.

The survey area is of low flat relief.

Weather conditions during the survey were typically cold (9°C) and partly cloudy with occasional showers. During the magnetic and radiometric survey, conditions were cold (0°C) and clear.

Figure 9: Aerial view of the survey area topography – Block V.

The survey block corner coordinates were provided by Waseco in NAD83 zone 19N UTM easting and northing. The following tables contain the survey block corner coordinates in NAD83.

Table 7: Waseco Resources Inc. - Block V – Lac Wawiyusi Anatwayach Survey Area Description

Lac Wawiyusi Antawayach Block V		
Corner	UTM Easting	UTM Northing
1	441306	6206490
2	441356	6210205
3	444472	6210164
4	444424	6206454

Coverage Type (%)			
Boreal Forest	Tundra	Marshland	Outcrop
20	50	15	15

The gravity stations were surveyed on rectangular grid at 500 m intervals.

The magnetic and radiometric surveys were surveyed along east-west flight lines with a line separation of 100 metres. Tie lines were flown north-south with a line separation of 1000 metres.

The Block V Survey Area covered a total of approximately 11 km².

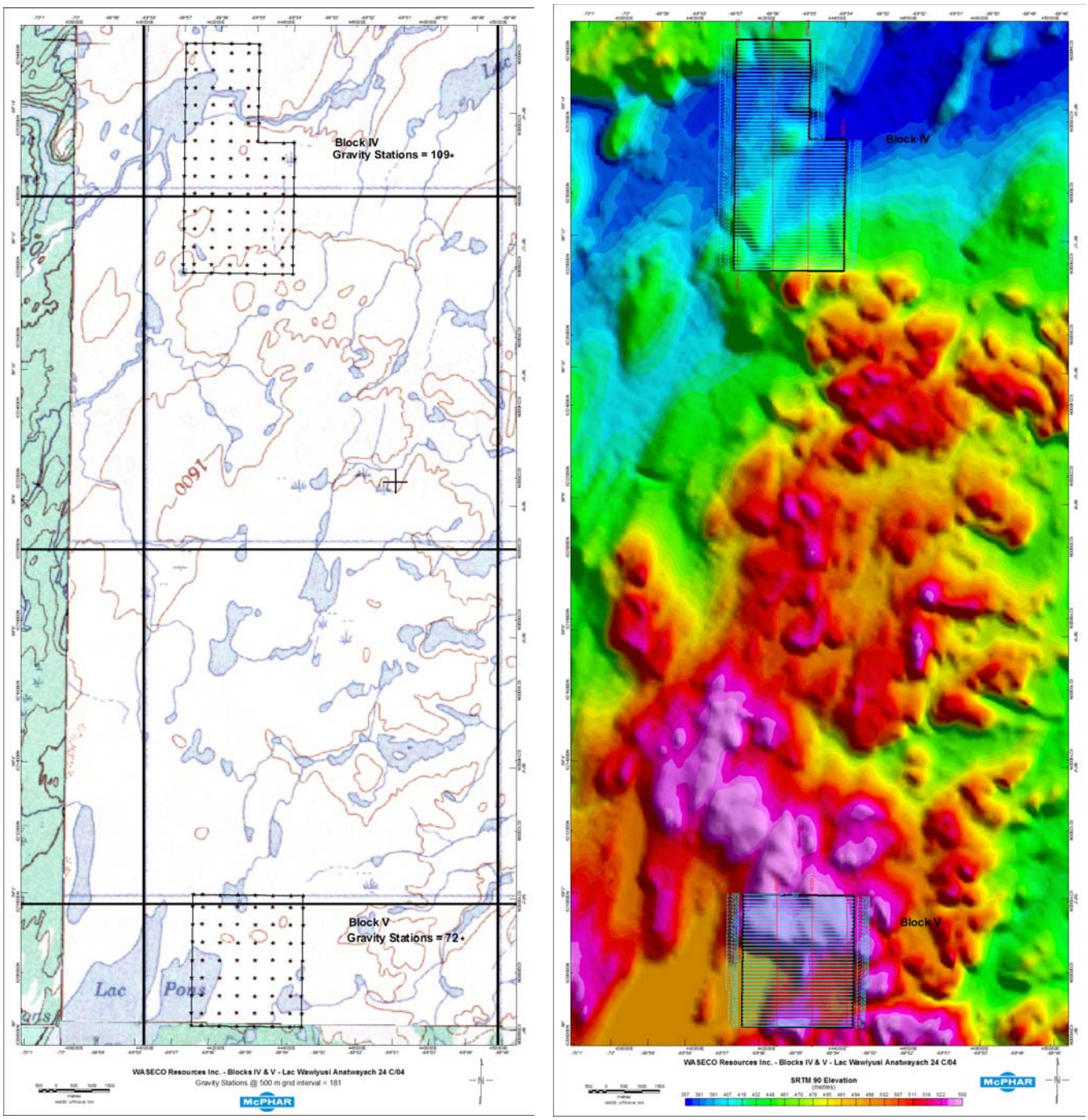

Figure 10: Block IV survey area with planned gravity stations and planned flight lines.

4. SURVEY OPERATIONS

4.1 Operations Base

Survey operations were based at the Lac Pau Lodge, Quebec, Canada, located approximately 130 km kilometres south of the survey area of Block V - Lac Wawiyusi Anatwayach and approximately 190 kilometres south-west of the Block I - Lac Bravo, Lac Crabe and Lac du Portage. Permission was obtained to operate and park the helicopter; locate, establish and operate the master gravity/GPS base station and GPS/magnetic base station was obtained from the owner of the Lac Pau Lodge. A Robinson R44 Raven helicopter owned and operated by ProspectAir was used for the transportation of the gravity crew and equipment to survey areas and for the subsequent airborne magnetic and radiometric surveys.

Figure 11: Arial view of Lac Pau Lodge operation base.

Quality Control and preliminary data processing was undertaken by the crew at the Lac Pau Lodge.

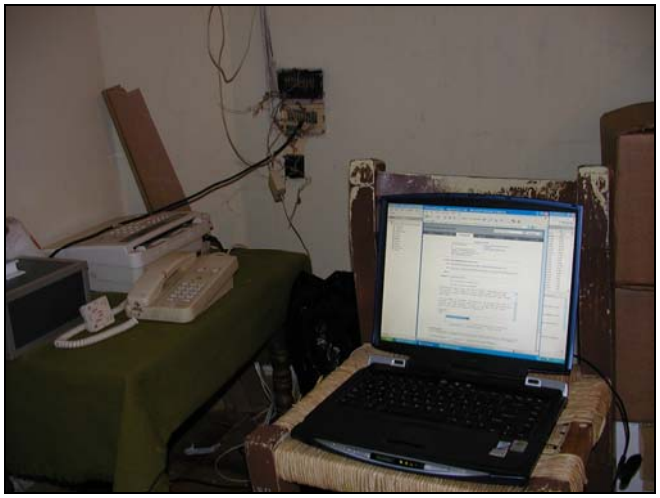

Figure 12: Field office in Lac Pau Lodge

Table 8: Distances between individual survey areas and operation base in kilometres

	Block A	Block B	Block C	Block D	Block E	Lac Pau Lodge
Block A		106	129	125	140	259
Block B	106		21	98	106	153
Block C	129	21		104	110	130
Block D	125	98	104		15	194
Block E	140	106	110	15		189

4.2 Survey Conditions

Weather conditions during the gravity survey were good with high overcast cloud conditions and occasional rain showers. Two days of the gravity survey were suspended due to rain and strong wind. Temperature was in the mid 10°'s Celsius over the course of the gravity survey.

Figure 13: Typical survey conditions for the gravity component of the project.

Survey conditions for the airborne magnetic and radiometric phase of the project were generally good, with overcast skies and cool temperatures in the 0^{o} Celsius to 5^{o} Celsius range.

4.3 Gravity Survey Technique / Methodology

The gravity / GPS survey was comprised of the following components:

- Calibration and tests of gravity meters and GPS receivers
- Establishment of a GPS Base Station network
- Establishment of a Gravity Base Station Network
- Gravity measurements on 500 m x 500 m gravity station grid
- GPS measurements on 500 m x 500 m gravity station grid
- Data quality control and preliminary data processing.

4.3.1 Establishment of GPS Base Stations

Five (5) GPS base stations were established for the project. One GPS base station was established approximately in the centre for each individual survey block (Block I, Block II, Block III, Block IV and Block V). As a result, no gravity / GPS station on the survey grid was further than ten (10) km from a GPS Base Station. All GPS Base stations were coincident with gravity base stations. A second, temporary, back-up base station was established close to each of the five GPS base stations for the purpose of backing up the data collected from the principal base station. Outage on the principal base stations was not registered during entire survey. Principal GPS base stations and back-up GPS base stations were placed on rocks and temporarily marked with colour.

The co-ordinates of each base station were determined using GPS data collected from a minimum of eight (8) satellites observed over a minimum period of 8 hours. The collected data were reduced using the TOPCON Tools software supplied with the GPS receivers.

An overview of the GPS Base Stations that are incorporated in the GPS Base Station Network has been provided as Table 8 below. The forms of GPS/Gravity stations are presented in Appendix 2.

Table 9: GPS Base Station Details for WGS84 Ellipsoid

Base Stn. #	Latitude [dd mm ss.ssss]	Longitude [dd mm ss.ssss]	Ellipsoidal height [m]	Survey Block
901	57.09.38.1 S	69.48.07.5 W	434	Block III
902	56.13.22.6 S	69.55.36.8 W	399	Block IV
903	56.00.59.1 S	69.56.40.9 W	477	Block V
904	56.22.21.6 S	68.20.35.9 W	381	Block I
905	56.15.33.9 S	68.12.24.6 W	349	Block II

Figure 14: TOPCON HyperLite GPS receiver collecting data on GPS base station.

4.3.2 Establishment of a Gravity Base Station Network

A network of gravity base stations (GBSN) was established for this project, comprised of one (1) principal base station located at the Lac Pau Lodge operation base and 5 base stations located in 5 individual survey blocks.

The principal "A-Order" base station (# 900) was established at the Lac Pau Lodge operation base. Base station 900 was not tied to the GSC gravity network, as the GSC gravity base stations established in the area in 1972 could not be located in the field and were assumed to destroyed or currently underwater. A fixed value of 980,000.00 mGal was used for the principal gravity base station. This value was used in the reduction of all gravity data collected during this survey and therefore the gravity values should be considered as relative values to this reference and not as absolute gravity observations.

One "B-Order" gravity base station was established in the approximate centre of each survey block. A total of five (5) "B-Order" gravity stations were established and tied to principal gravity base station as the survey progressed by completing several loops utilizing the same LaCoste & Romberg gravity meter (serial number G-1011).

The list of all base station loops including calibration lines surveyed on this project is included as part

of Appendix 2.

Gravity data from the Gravity Base Stations were processed using custom scripts running under GEOSOFT Oasis/Montaj software.

The results of gravity base stations tie survey are included as part of Appendix 2.

An overview of the Gravity Base Station statistics as incorporated to produce the Gravity Base Station Network for Waseco project is included as Table 10.

Table 10: Overview of the six Gravity Base Stations

Gravity Base Station #	Gravity Value	Method of determination	Survey Block	Standard Deviation
900	980 000.000	Fixed	Lac Pau Lodge	n/a
901	980 196.016	Surveyed	Block A	0.037
902	980 123.305	Surveyed	Block B	0.024
903	980 096.743	Surveyed	Block C	0.018
904	980 119.492	Surveyed	Block D	0.020
905	980 115.448	Surveyed	Block E	0.014

Figure 15: Gravity operator taking reading at gravity base station 900 at the Lac Pau Lodge.

4.3.3 Gravity Survey Logistics

The survey was carried out by three (3) gravity / GPS operators. The operators were divided into two (2) gravity crews, each gravity crew consisting of one (1) gravity operator. Each gravity crew was equipped with the following equipment: one (1) gravity meter; one (1) GPS/ROVER receiver; one (1) GPS handheld receiver and one (1) compass.

The gravity stations were surveyed on ground. A Robinson R44 Raven helicopter was used for gravity crew transportation from the Lac Pau Lodge operation base to the survey area and from gravity station to gravity station where possible. Some areas of some survey blocks were covered by thick forest with high trees or by large areas of muskeg which negated use of the helicopter for gravity station to gravity station moves. These areas encompassed approximately thirty five percent (35%) of the gravity stations to be surveyed and could only be accessed on foot from the closest helicopter access point.

Communications between the helicopter and gravity crews and between the helicopter and the Lac Pau Lodge was maintained through the use of handheld FM-radios.

4.3.4 Navigation

Navigation was assisted through use of a GPS handheld receiver that reporting GPS co-ordinates in units of WGS-84 latitude and longitude. These coordinates were also pre-programmed as a two-dimensional (2-D) survey grid into the helicopter navigation system for pilot navigation.

The gravity ground survey crews then navigated by handheld GPS and compass to within a 50-metre radius of the ideal grid location. At this location, reception from a minimum of 6 GPS satellites maintained. For surveying purposes, the coordinates of the survey area were transformed from WGS84 Geographic coordinates to projected NAD83 Zone 19N coordinates.

4.3.5 Gravity Survey Measurements

4.3.5.1 Daily Loop Measurements

All gravity stations were surveyed in loops starting and ending from the appropriate “B-Order” base station for a given survey block. The average time length between start and end (closure) on a gravity survey loop was 6 hours.

A “loop” is the basic component of a gravity survey. A loop consists of a sequence of gravity observations, commencing from and including a known gravity control point (base station) and ending on a known gravity control point.

4.3.5.2 Placing of the Gravity Meter on Station Locations

The gravity meter was placed a maximum of 10 cm from the bipod location of the GPS antenna. The Vertical Instrument Height was measured from the bottom of the gravity meter to the ground and was recorded in the field notebook by the operator.

4.3.5.3 Readings on Gravity Stations

At each gravity station at least two (2) successive readings were obtained. If these two (2) readings differed by more than 0.01 mGal, additional successive readings were obtained. The final reading value was obtained by calculating the average of all successive readings for a given visit by the operator and recorded in the field notebooks. By following this procedure it was possible to increase the accuracy of the gravity values measured at each station.

4.3.6 GPS Survey Measurements

All gravity stations were surveyed using dual-frequency geodetic quality GPS receivers. The GPS systems used were the TOPCON HyperLite model (specifications in Appendix 4). The differential GPS (fast-static post-processing) survey mode was used to collect all GPS data. Every effort was made by the Gravity / GPS operators to locate the gravity stations at sites where the best possible satellite coverage (minimum 6-8 satellites) could be obtained.

To meet the proposed GPS accuracy (+/- 5 cm + 1-2 ppm), all stations were surveyed within a 10 km radius of a GPS Base Station. The GPS observation time on station to obtain the specified accuracy required a minimum period of ten (10) minutes, dependent on the number of satellites visible to the GPS unit at the time of measurement.

Both the base station GPS readings and the Rover GPS readings were collected at a frequency of one (1) sample for every four (4) seconds. The height of the antenna above the ground at the stations was measured using the scale on the bipod -pole. The GPS antenna height and recording time was noted by the operator in his field notebook.

At the end of each survey day the raw GPS data was downloaded from each of the GPS receivers and transferred to the QA/QC data processor at the Lac Pau Lodge operations centre. GPS data reduction and processing was completed on a daily basis.

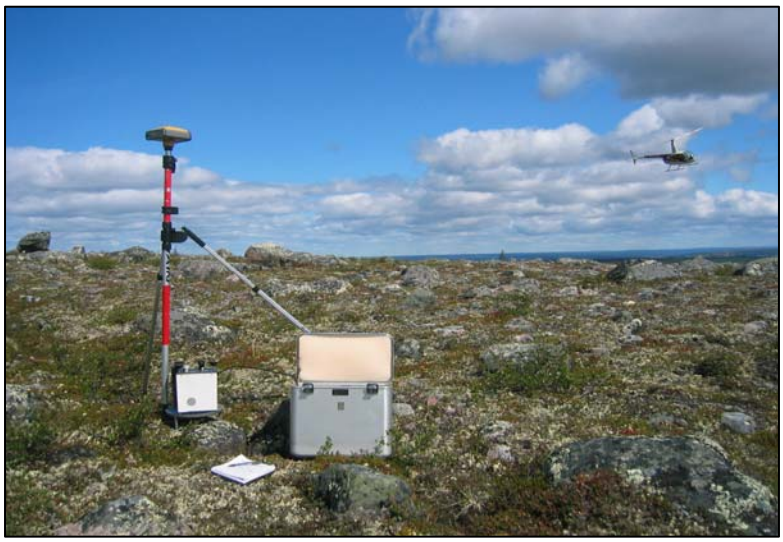

Figure 16: LaCoste & Romberg Gravity meter and TOPCON GPS receiver in field use.

4.3.7 Gravity Survey Field Data Processing & Quality Control

At the end of the each survey day, the positioning data was downloaded from the GPS receivers and the gravity data recorded in the operator's field notebook was transferred to the data processor for Quality Control and data processing. The QC and data processing is described in detail in section 6 of this report.

In-field data processing included the reduction of the data to GEOSOFT GDB database format and inspection of the all recorded data for adherence to contract specifications. Survey stations that exhibited excessive deviation after differential correction, or that were considered to be of inferior quality, were marked to be resurveyed.

4.3.8 Gravity Survey Statistics and Project Diary

The gravity survey entailed a total of 70 flights of which 28 flights were production flights. The first production flight was Flt #05 on 23 June 2005; the last production flight was Flt #68 on 8 July 2005. The gravity project dairy is presented in table below, the complete flight time data and other operations data are included as part of Appendix 2.

Table 11: Gravity Project Diary

Date	Flt #	Hours Flown	Stations Accepted	Comments
19 – 21 June	1	8.5		Crew mobilized by road with all survey equipment from Newmarket, Ontario, arriving in Lac Pau Lodge in the afternoon. Helicopter ferried from Gatenau, Quebec to Lac Pau Lodge
22 June	2, 3	0.5		Could not fly till afternoon due to high gusty winds. Tried to locate GGSC gravity base station in afternoon. Appears that marker has been flooded since dam was built in 1978. Operation base, field data processing centre and principal gravity base was established at camp Lac Pau Lodge.
23 June	4, 5	8.1	32	Survey commencement in Block C.
24 June	6 to 10 inclusive	8.0	31	Survey in Block C completed. Gravity base station 902 in Block B established.
25 June	11 to 14 inclusive	10.3	51	Survey commencement in Block B
26 June	15 to 19 inclusive	8.8	34	Survey continuation in Block B. Tried to locate another GSC gravity base station – likely the marker was destroyed
27 June	20 to 24 inclusive	8.9	34	Survey in Block B completed Gravity base station 901 in Block A established Survey commencement in Block A
28 June	25 to 32 inclusive	10.2	43	Survey in Block A completed
29 June	33 to 37 inclusive	9.0	39	Survey commencement in Block D

Date	Flt #	Hours Flown	Stations Accepted	Comments
30 June	38 to 41 inclusive	9.2	31	Survey continuation in Block D.
1. July				Stand by – heavy rain
2. July	42 to 46 inclusive	7.5	33	Survey continuation in Block D.
3. July	47 to 50 inclusive	5.3	13	Survey continuation in Block D. Half day of production due to rain
4. July				Stand by – due to rain
5. July	51 to 55 inclusive	11.2	61	Survey continuation in Block D.
6. July	56 to 61 inclusive	10.3	59	Survey in Block D completed Gravity base station 906 in Block E established
7. July	62 to 65 inclusive	10.1	52	Survey commencement in Block E
8. July	66 to 70 inclusive	8.1	24	Survey in Block E completed. Repeat stations in Block D surveyed
9. July				Crew and equipment demobilization
Totals		**134**	**539**	

A total sixty five percent (65 %) of the gravity stations were directly accessible by helicopter. The remaining thirty-five percent (35%) of the gravity stations could only be accessed on foot. The details of station accessibility are presented in Table 12.

Table 12: Overview of Gravity Station Accessibility by Helicopter

Accessibility with Helicopter from Ideal Planed Location of the Gravity Station		
Within radius of 50m	Within radius of 200m	Out of radius of 300m
95 %	5 %	-
60 %	35 %	5 %
65 %	30 %	5 %
55 %	30 %	15 %
50 %	35 %	15 %
65 %	27 %	8 %

Total 569 discrete gravity stations were preplanned for the projct and an actual total 539 discrete stations were measured by gravity and GPS. A total 30 gravity stations were not possible to be located during the survey due to difficult access or unsuitable ground conditions that prevented the acquisition of gravity or GPS observations to within survey specification. The surveyed gravity station statistics of preplanned versus actual are summarised in Table 13.

A total 38 gravity repeat readings were completed on 37 discrete gravity stations across all of the survey blocks to determine the accuracy of gravity survey.

Figure 17: Helicopter R44 landing close to gravity station in Block I

Table 13: Projected Versus Actual Measured Gravity Stations

Survey Block	Date of Survey	Number of Projected Gravity Stations	Number of Measured Gravity Stations	Number of Skipped Gravity Stations	Number of Repeats	Percentage of Repeats
A	27 - 28 June 2005	63	63	0	4	6.35%
B	25 -27 June 2005	109	100	9	6	6.00%
C	23 - 24 June 2005	72	63	9	10	15.87%
D	29 June - 6 July 2005	241	238	3	12	5.04%
E	7 - 8 July 2005	84	75	9	6	8.00%
PROJECT	23 June - 8 July 2005	569	539	30	38	7.05%

The following personnel were the onsite crew on the project in Lac Pau Lodge, Quebec:

Table 14: Gravity Survey Field Personnel

Title	Name	Days Onsite
Project Manager / Geophysical Technician	Dallas Antill	18
Operator / Gravity QC Geophysicist	Juraj Kovacik	18
Operator / GPS QC Geophysicist	Juraj Vanik	18
Helicopter Pilot	Alan Trombley	19

McPhar Geosurveys Ltd. of Newmarket, Ontario, Canada, was responsible for the field operations and the overall coordination and management of the gravity survey.

Figure 18: Crew in front Helicopter R44 at Lac Pau Lodge operation base.

4.4 Magnetic and Radiometric Survey Technique / Methodology

The airborne magnetic and radiometric survey was comprised of the following components:

- Testing of the towed bird magnetic sensor
- Calibration and testing of the radiometric system
- Establishment of a magnetic / GPS Base Station
- Acquisition of magnetic and radiometric data over the survey blocks on 100 m separation flight lines and 1000 m separation tie lines
- Data quality control and preliminary data processing.

4.4.1 Magnetic / GPS Base Station

A magnetic and GPS base station was established at the Lac Pau Lodge for the duration of the airborne magnetic and radiometric survey. The site selected for the base station was magnetically quiet and removed from sources of cultural magnetic noise and radio frequency interference. The site also afforded excellent GPS satellite visibility with a minimum of 6 to 8 satellites in view at any one time.

The base station was operated for continuously over the duration of the survey, the only periods of non acquisition occurring when the data was being retrieved from the datalogger at the end of a given days survey activity.

The base GPS data was acquired as a redundant backup to be utilised if necessary should the real time correction of the aircraft system have failed.

4.4.2 Magnetic and Radiometric Survey Logistics

In an effort to optimise survey production, three (3) fuel caches were established in the survey block areas. Fuel was flown into Blocks I and II, Block III and Blocks IV and V via float plane chartered from Air Saguenay. Upon completion of the survey, the spent fuel drums were retrieved.

Figure 19: Air Saguenay float plane (left) and remote fuelling of the R44 on the lakeshore, Block IV (right).

The radiometric system calibration and pre and post flight tests were completed on a twice daily basis at the Lac Pau Lodge operations base. Weight and fuel imposed restrictions with the Robinson R44 helicopter precluded the presence of an operator on board during the survey flying. All survey data acquisition systems were operated in flight by the pilot of the helicopter.

Regular flight following and technical assistance while the helicopter was on survey was maintained through use of FM-radio communication and/or satellite telephone communication with the Lac Pau Lodge operations base.

4.4.3 Navigation

The nominal data acquisition speed of the helicopter was approximately 110 kilometres per hour. Scan rates for magnetic data acquisition was 0.04 seconds (25 Hz), 1.0 second (1 Hz) for the spectrometer and radar altimeter, and 1.0 second (1 Hz) for the GPS navigation/positioning system. Therefore, a magnetic value was recorded approximately every 1.2 meters and a position fix every 30 meters along the flight track.

Navigation was assisted by a GPS receiver system that reported GPS co-ordinates as WGS-84 latitude and longitude and directed the pilot over a pre-programmed two-dimensional (2-D) survey grid. The x-y-z position of the aircraft as reported by the GPS system and terrain clearance determined from the radar altimeter was recorded on the data acquisition systems. For surveying purposes, the coordinates of the survey area were transformed from WGS84 Geographic coordinates to projected NAD83 Zone 19N coordinates.

Vertical navigation along flight lines was established using the radar altimeter. The optimum terrain clearance during normal survey flying was 50 metre for the helicopter and radiometric system, 25 metre for the towed-bird magnetometer. However, at all time during the survey, the pilot's judgment of safe flying conditions was the final arbiter in the determination of safe terrain clearance and hence the contract specification may not have been not possible 100% of the time.

The final vertical and horizontal survey positions were real time corrected in flight to a precision of approximately +/- 1.5 metre.

4.4.4 Magnetic and Radiometric Field Processing and Quality Control

Daily radiometric sample checks were performed to determine proper operation of the aircraft radiometric system.

All survey data was transferred to portable magnetic media on a flight-by-flight basis, and then copied to the field data processing workstation. In-field data processing included reduction of the data to GEOSOFT GDB database format and inspection of the magnetometer data for adherence to contract specifications. Survey lines that exhibited excessive deviation after differential correction, or that were considered to be of inferior quality, were marked to be reflown.

Several flight lines were flown in segments due to wind conditions. When this occurred, an overlap between line segments of a minimum of two tie lines was maintained.

4.4.5 Magnetic and Radiometric Survey Statistics and Project Diary

The survey entailed a total of 3 production flights. The first production flight was on 14 September 2005, with the last production flight on 16 September 2005.

Table 15: Airborne Magnetic and Radiometric Project Diary

Date	Flt #	Hours Flown	Line-Km Accepted	Comments
12 Sept.				Crew mobilized by fixed –wing and helicopter to Lac Pau Lodge
13 Sept.				Magnetic base station established, helicopter systems tested.
14 Sept.	1			Flying of Block V completed and equipment calibrations flown.
15 Sept.	2			Flying of Block III and IV completed.
16 Sept.	3			Flying of Block I and II completed.
17 Sept.				Crew demobilised from Lac Pau Lodge.

Table 16: Airborne Magnetic and Radiometric Survey Field Personnel

Title	Name	Days Onsite
Project Manager / Geophysical Technician	Barry Levy	6
Geophysical Technician	Kevin Lindsay	6
Helicopter Pilot	Alan Trombley	6

5. HELICOPTER AND EQUIPMENT

5.1 The Helicopter

The survey was flown using a Robinson R44 Raven helicopter, with Canadian registration C – GLMD provided by Prospect Air of Quebec. This helicopter featured up to 5 hours flight duration with the geophysical equipment and a crew of 2 persons onboard.

The gravity survey did not require the installation of any additional geophysical equipment into the helicopter.

The installation of the magnetic and radiometric and ancillary equipment was completed by McPhar and Prospect Air personnel at the Gatineau, Quebec facilities of Prospect Air prior to mobilisation to Lac Pau Lodge. Final adjustments, calibration and testing were completed prior to production survey flights commencing from the Lac Pau Lodge operations base.

Aircraft Registration:	-	Canadian, C-GLMO
Engine:	-	Textron Lycoming – 0-540-FIBS - 245 hp
Empty weight:	-	1,442 lbs / 655 kg
Gross weight:	-	2,400 lbs / 1,088 kg
Max cruise:	-	113 knots / 205 kph
HIGE:	-	6,400 ft / 1,969 m
HOGE:	-	5,100 ft / 1,569 m
Service ceiling:	-	14,000 ft / 4,308 m
Standard fuel:	-	49 gal /187 litres
Survey duration:	-	4.0 hours
Maximum range:	-	approx. 400 miles (640 km)

Figure 20: Helicopter C-GLMO with magnetic sensor bird.

Figure 21: Helicopter Robinson R44 Raven taking-off from Lac Pau Lodge.

5.2 Gravity Survey Instrumentation Overview

The instrumentation used for the Waseco gravity survey included:

- Two (2) Lacoste & Romberg Model G Land Gravity Meters
- Four (4) TOPCON HyperLite GPS Systems
- Three (3) Magellan eXplorist portable handheld GPS receivers

5.2.1 LaCoste & Romberg Gravity Meters

The LaCoste & Romberg model-G has a world-wide range of 7,000 milliGals, and is a standard in gravity surveys world-wide. The LaCoste & Romberg model-D has a range of 200 milliGals The L&R meters are a rugged, robust field instruments, designed to meet the demands of normal field operation while retaining the highest data quality. The G-meter has a repeatability of 0.01 milliGal and an accuracy of better than 0.05 milliGal. The D-meter has a repeatability of 0.005 milliGal and an accuracy of better than 0.02 milliGal. The sensing element of the L&R meter is based on a zero length

spring and a lever system is used to null the meter. The gravity responsive system of the L&R-meter is completely suspended by springs and will normally withstand any shock that will not damage the supporting housings. The L&R model-G is described in Appendix 3.

Figure 22: LaCoste & Romberg Model G Land Gravity Meter

Table 17: Land Gravity Meters used on the Waseco Project

Gravimeter No.	Make & Model	Serial No.
1	LaCoste & Romberg	G-1011
2	LaCoste & Romberg	D-180

5.2.2 TOPCON HyperLite GPS Systems

Figure 23: TOPCON HyperLite GPS System

TOPCON's HyperLite GPS System is an integrated, compact system for high-accuracy post-processed and real-time GPS surveying. It may also be optionally configured with a GLONASS receiver.

The TOPCON HyperLite is a small, lightweight, totally integrated GPS system, combining a 12-channel, dual-frequency L1/L2 GPS receiver, Lithium Ion battery with up to 14-hours life, with integrated internal memory upgradeable up to 1 GB, and an internal radio data link into one small unit. The Topcon HyperLite is a portable system that allows centimetre-accurate surveying.

Two TOPCON HyperLite GPS systems were used as "Rovers" and two TOPCON HyperLite GPS systems used as bas stations on this project.

Table 18: Dual Frequency Geodetic GPS Systems used on the Waseco Project

GPS System No.	Make & Model	Serial No.
1	TOPCON HyperLite	263-0460
2	TOPCON HyperLite +	295-1156
3	TOPCON HyperLite	263-0428
4	TOPCON HyperLite +	295-1174

Full details of the TOPCON HyperLite are included as part of Appendix 3.

5.2.3 Magellan eXplorist GPS Receivers

The Magellan eXplorist is a lightweight, rugged, waterproof handheld GPS navigator. The units had a large and easily readable 16-colour display and a front facing 9 key keypad. The units included 8 MB of memory with additional data storage capacity available via a secure digital (SD) card.

The accompanying SporTrak software included 9 graphic navigation screens, storage for up to 500 waypoints and 20 routes with BackTrack software for returning to the starting point along the same route. The units were capable of WAAS accurate positioning.

Full details of the Magellan eXplorist are provided in Appendix 3.

Figure 24: Magellan eXplorist GPS Receiver

5.3 Magnetic and Radiometric Survey Instrumentation Overview

The instrumentation installed in the helicopter for the magnetic and radiometric survey included:

- A Geometrics G822A high-sensitivity Cesium magnetometer mounted in a towed-bird airfoil, 0.001 nT / 10 Hz resolution
- A Pico-Envirotec GRS-410 self-stabilizing multi-channel gamma-ray spectrometer with 33.6 litres "downward looking" NaI sensor, temperature and barometric pressure probes.
- An AGIS Data Acquisition System
- A navigation system, comprising an Fugro 3000 OmniStar DGPS receiver and AGNAV GPS computer with pilot steering indicator (PSI)
- A T.H.E.M. Geophysics Data Acquisition System (DAS)
- A Terra TRA-3000/TRI-30 Radar Altimeter

The magnetic and GPS base station comprised:

- A Magnetometer / GPS Base Station, comprising a PC-based DAS base station magnetometer and GPS system.

A complement of spare parts and test equipment were maintained at the survey site.

5.3.1 Airborne Magnetometer

A Geometrics G822A cesium split-beam total-field magnetometer was installed in the Kevlar airfoil. Sampling rate was nominally twenty-five (25) times per second with an in-flight sensitivity of 0.01 nT. Aerodynamic magnetometer noise was less than 0.25 nT. The sensitivity of the magnetometer is recorded at 0.001 nT when operated at a sampling rate of 0.1 second.

The Geometrics G-822A magnetometer is described in Appendix 3.

Figure 25: Geometrics G-822A cesium magnetometer

5.3.2 Gamma-ray Spectrometer System

The gamma ray system included a Pico-Envirotec GRS-410 multi-channel gamma-ray spectrometer with 33.6 litres of "downward looking" NaI sensor with a sampling rate of 1 second. The thermally isolated NaI crystal sensors were installed in the cabin of the helicopter.

The GRS-410 is a 512 channel, self-stabilizing spectrometer that tracks and corrects for the spectral drift of the system by following a Thorium spectral peak. The standard regions of interest for Total Count (TC), Potassium (K), Uranium (U), Thorium (Th) and cosmic radiation were recorded for post survey processing. The averages recorded with window limits in MeV are shown in the following table:

Table 19: Standard Gamma-ray Spectrometer Data Acquisition Windows

Standard Gamma-ray Spectrometer Data Acquisition Windows		
Element	Lower Boundary (MeV)	Upper Boundary (MeV)
Total Count	0.41	2.81
Potassium	1.37	1.57
Uranium	1.66	1.86
Thorium	2.41	2.81
Cosmic	3.00	∞
Upward-looking Uranium	1.66	1.86

The spectrometer was calibrated on a daily basis using standard calibration sources for Thorium (Th), Cesium (Cs) and Uranium (U).

The recommendations in the International Atomic Energy Agency – IAEA – TECDOC-1363 – *Guidelines for radioelement mapping using gamma ray spectrometry* were followed throughout the survey.

5.3.3 The Towed-Bird Airfoil and Tow-Cable

The towed-bird airfoil is essentially a hollow Kevlar tube, 1.8 meters long, with a bulbous nose into which the cesium magnetometer sensor is mounted in a 3D hand-aligned gimbal. Fins are used at the tail of the airfoil to stabilize the bird in flight.

The tow cable is constructed of coaxial cables complete with a strain member. The length of the tow cable is nominally 30 metres. The tow cable was attached to the helicopter by a weak link assembly. The on-board section of the tow cable consists of a coaxial cable, the length customized to suit the helicopter.

Figure 26: Geometric G-822A cesium magnetometer mounted in the towed-bird airfoil.

5.3.4 The Base Station Magnetometer

The magnetometer base station used was comprised of a PC-based computer utilizing a Geometrics G-822A Cesium magnetometer to monitor and record diurnal variations of the Earth's magnetic field. The base station magnetometer was set up at the Lac Pau Lodge operations base. Every effort was made to ensure that the magnetometer sensor was placed in a location with a low magnetic gradient and sited away from electric transmission lines, and moving ferrous objects, such as motor vehicles and aircraft,

without compromising safety and aircraft operations.

The base-station magnetometer, with digital recording, was operated continuously throughout the airborne data acquisition work with a sensitivity of 0.01 nT. The ground and airborne system clocks were synchronised using GPS time, to an accuracy of 1 second or better. The sample rate was once per second. A continuously updated profile plot of the base station values was presented on the base station screen. At the end of the day, the digital data was transferred from the base station's data-logger to the fieldwork station.

Specifications are included in Appendix 3.

5.3.5 Altimeter

A Terra TRA-3000/TRI-30 radar altimeter was used to record terrain clearance to an accuracy of about 1 ft (30 cm), over a range of 12 metres to 762 metres. The antenna was mounted beneath the bubble of the helicopter cockpit. The recorded value of terrain clearance was adjusted to give bird height above ground. This was possible given the fixed tow cable length of 30 metres.

The altimeter was interfaced to the data acquisition system with an output repetition rate of 0.1 second, and digitally recorded.

The altimeter specifications are further described in Appendix 3.

5.3.6 The GPS Satellite Navigation System

An OmniStar DGPS receiver coupled with a CSI-Wireless DGPS navigation system input to a Pico-Envirotec AGNAV navigation computer and pilot steering indicator (PSI) provided in-flight real-time navigation control. A pilot steering indicator (PSI) installed on top of the cockpit dashboard, in front of the pilot provided steering and cross-track guidance to the pilot. The pilot was provided with GPS, and altimeter data to aid in flying the helicopter.

This navigation system yielded a real-time positional accuracy of better than ± 2 metre.

Survey co-ordinates were set-up prior to commencement of the survey, the information fed into the airborne navigation system. The co-ordinate system employed in the survey design and digital recording was WGS-84 latitude and longitude. The GPS positional data was recorded at one-second intervals and used with the base station data to calculate differentially corrected locations.

The GPS receiver is fully described in Appendix 3.

5.3.7 Data Acquisition/Recording System

A PC-based T.H.E.M data acquisition system (DAS) was used to record the magnetic and navigation survey data on an internal hard disk drive. A PC-based AGIS-100 data acquisition system (DAS) was used to record the radiometric and navigation survey data onto an internal hard disk drive. Both DAS systems displayed data on an LCD screen as traces to allow the operator to monitor the integrity of the system. The DAS provided for the:

- System control and monitoring
- Data acquisition recording
- Real-time data processing
- Navigation processing, and
- Post flight data playback and analysis

All data collection routines, checking and verification, buffering, and recording are software controlled for maximum flexibility both during and after the survey flight.

The DAS are described in Appendix 3.

5.4 Field Computer Workstations

A Data Processing Field Workstation (FWS) comprised of a dedicated PC-based notebook computer for use at the technical base in the field, was used on this project. The FWS is designed for use with GEOSOFT OASIS/Montaj Data Processing Software. The FWS has a data replot capability, and may be used to produce pseudo-analogue charts from the recorded digital data within less than 12 hours after the completion of a daily survey production, if this is necessary. It is also capable of processing and imaging all the geophysical and navigation data acquired during the survey, producing semi-final, preliminary-reduced maps.

The FWS was used to accomplish the following:

- **Quality Control/Digital Data Verification** – gravity and GPS data quality and completeness were assured by both statistical and graphical means on a daily basis
- **Station Position Plots** – station position plots and flight path plots were generated from the GPS satellite data to verify the completeness and accuracy of each day's production
- **Preliminary Maps -** the Geosoft software system permitted preliminary maps to be quickly and efficiently created for noise and coherency checks.

The FWS is fully described in Appendix 3.

The GEOSOFT OASIS/Montaj software is designed for airborne data editing, compilation, processing and plotting. The software reads the portable data media from the airborne system checks them for gaps, spikes or other defects and permits the data to be edited where necessary. The base station GPS/magnetometer data is checked, edited, processed and then merged with the airborne data. GPS flight path plots are created and plotted for both flight planning and flight path verification.

5.4.1 Spares

A normal compliment of spare parts, tools, back-up software, and necessary test instrumentation were available in the office at the operation base.

6. INSTRUMENT CHECKS AND CALIBRATIONS

6.1 Gravity Meter Tests and Calibrations

6.1.1 Instrument Calibrations

Two LaCoste & Romberg gravity meters with serial numbers G-1011 (Gravity meter # 1) and D-180 (gravity meter # 2) arrived Lac Pau Lodge on 21 June 2005. The gravity meters were temperature stabilized over a 72-hour period in the Newmarket office of McPhar prior to being transported by truck to the Lac Pau Lodge. Both gravity meters underwent the manufacturer's recommended stabilization and set-up and calibration procedures (Appendix 3) prior to commencing survey operations.

6.1.2 Scale Factor Test

A network of gravity base stations (GBSN) was established for this project. The network was comprised of one (1) principal base station located at the Lac Pau Lodge and five (5) base stations; one base station located on each of the five (5) survey blocks.

Gravity base stations 901, 902, 903, 904 and 905, were used to test and verify the gravity meter scale factors. The calibration test was undertaken during the survey through the measurement of three (3) calibration lines:

1. Calibration line between base stations 901 and 902 - range of 72.69 mGal
2. Calibration line between base stations 902 and 903 - range of 26.54 mGal
3. Calibration line between base stations 904 and 905 - range of 4.04 mGal

The calibration lines were surveyed using both gravity meters, by performing a closed loop survey as outlined by Figure 27.

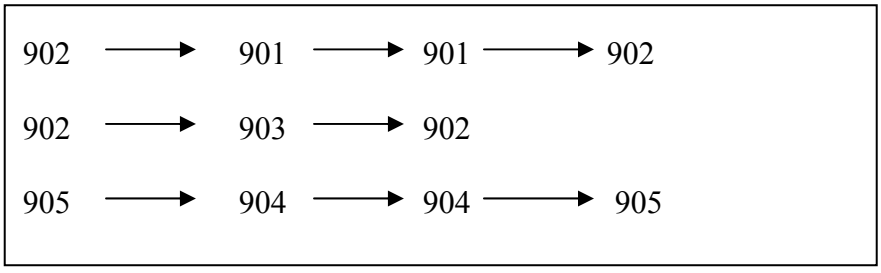

Figure 27: Diagram of gravity meter calibration loops.

The list of all base station loops including the calibration lines are included as part of Appendix 2.

Results obtained from the base station loop / calibration lines confirmed that scale factor tables as provided by the manufacturer were valid for both gravity meters G-1011 and D-108. The Standard Deviation (SD) of gravity of all three (3) gravity ranges was within specification. The maximum dispersion as defined by the SD was 0.021 mGal for the calibration range of 72.69 mGal between base stations 901 and 902. The results of scale factor test are included as part of Appendix 2.

6.2 Gravity Survey GPS Static Test

Care was taken to ensure that the exact position of the GPS base station was determined. The base GPS system data was averaged over a period of time to calculate the location coordinates. The base station GPS had a maximum field-of-view at all times to the NAVSTAR satellites.

6.3 Airborne Magnetic System Tests and Calibrations

6.3.1 Magnetic Heading Effect

The magnetic heading effect was determined by flying a cloverleaf pattern oriented in the same direction as the survey lines and tie lines. Two passes in each direction were flown over a recognizable feature on the ground in order to obtain sufficient statistical information to estimate the heading error. The heading error was determined from a test completed on 13 September 2005. The results of the heading test are presented in Appendix 2.

6.3.2 Lag Test

A Lag Test was performed on 13 September 2005 to ascertain the time difference between the magnetometer readings and the operation of the GPS System. The test was flown over an identifiable magnetic anomaly by flying the same line in opposite directions at survey altitude. The lag test is included in Appendix 2.

6.4 Airborne Gamma-ray Spectrometer System Tests and Calibrations

6.4.1 Test Line

A test line was flown and recorded at survey altitude at the start and end of each survey flight to test the repeatability of the gamma-ray spectrometer system. The minimum, maximum and average deviation for each of the four windows (TC, U, Th and K) was calculated and stored in a database for future reference and use. The results of flying the test line are included in Appendix 2.

6.4.2 Altitude Attenuation Coefficient

The altitude attenuation coefficient was derived from a test flight completed on 13 September 2005 prior to commencement of the survey. This was accomplished by flying a test line at various altitudes from 200' (63 m) up to 1,000' (305 m) above the test line. The coefficients used are included in Appendix 2.

6.4.3 Cosmic Window Calibrations

Cosmic window calibrations or Background Attenuation Coefficients were measured and calculated for the detector crystal packs on 13 September 2005. The coefficients were calculated from a sequence of

passes flown at various altitudes above the ground (altitudes of approximately 610 m, 914 m, 1220 m, 1372 m and 1524 m) with each altitude flown for a minimum of 2 minutes.

The average values of the counts measured in each of the 4 windows (TC, U, Th and K) are compared against the average counts for the cosmic window at each of the altitudes flown. The results of the calibration test flights are presented in Appendix 2.

6.4.4 Spectral Resolution Test

The resolution of the spectrometer was determined before and after each survey flight, using the 662 keV gamma rays from a Cs^{137} source. The pre flight measurements were to be completed after any detector gain adjustments had been applied. The post flight measurement was to be completed without any gain adjustment being made. The results of this test are presented in Appendix 2.

6.4.5 Daily Source Checks

The spectrometer was calibrated before the first survey flight of the day and after the last survey flight of the day using standard calibration sources, comprised of Cesium (Cs137), Uranium (Bi214) and Thorium (Th208). A background measurement was recorded, then each of the sources individually recorded, followed by a final background measurement. Each measurement was for a duration of 60 seconds. The sources were placed in exactly the same position relative to the gamma-ray sensors each time the source checks were completed. The results of this test are included in Appendix 2.

6.5 Altimeter Calibration Checks

Altimeter test flight was performed on 13 September 2005. The radar altimeter was calibrated by comparing the radar altitude with a suitable reading from the GPS navigation system during radar "stack" flown over the Lac Pau Lodge helipad. The ellipsoidal height at this location on the Lac Pau Lodge helipad was determined by GPS. The procedure involved having the helicopter hover for 30 seconds at various altitudes above the ground (45, 60, 76, 91 and 152 metres) and recording the values of the radar altimeter and GPS altimeter. These values were then plotted and compared. The results of the test are included in Appendix 2. The radar calibration was checked on a daily basis by completing a vertical calibration test flight during take off and landing.

6.6 GPS Static Test

In addition to carefully selecting a magnetically suitable area for positioning the magnetometer base station, care was taken to ensure that the exact position of the GPS base station was determined. The base GPS system data was averaged over a period of time to calculate the location coordinates. The base station GPS had a maximum field-of-view at all times to the NAVSTAR satellites.

7. QC AND DATA PROCESSING

Daily quality control, initial processing and archiving of the gravity, aeromagnetic and radiometric data were completed on-site at the base of operations at the Lac Pau Lodge accommodations using Geosoft Oasis/MONTAJ software for the geophysical data and TOPCON TOOLS GPS post-processing software for the gravity survey GPS station locations. The software was installed on the FWS computers. All data were verified upon receipt, and checked against the operator's logs.

The Quality Control and Data Processing of the gravity survey data involved the following procedures:

a) Data quality control comprising of examination and checking of all incoming data to ensure completeness of data sets and data quality corresponding to contract specifications and industry standards.

b) Integrated data pre-processing of gravity and GPS data comprising of Differential GPS Data Processing, basic gravity reductions and corrections and production of preliminary gravity path maps.

c) Final data processing comprising of terrain correction calculation, precise Bouguer anomaly calculation and production of derivative maps. The final data processing, map generation and report was completed by McPhar at the Newmarket, Ontario office.

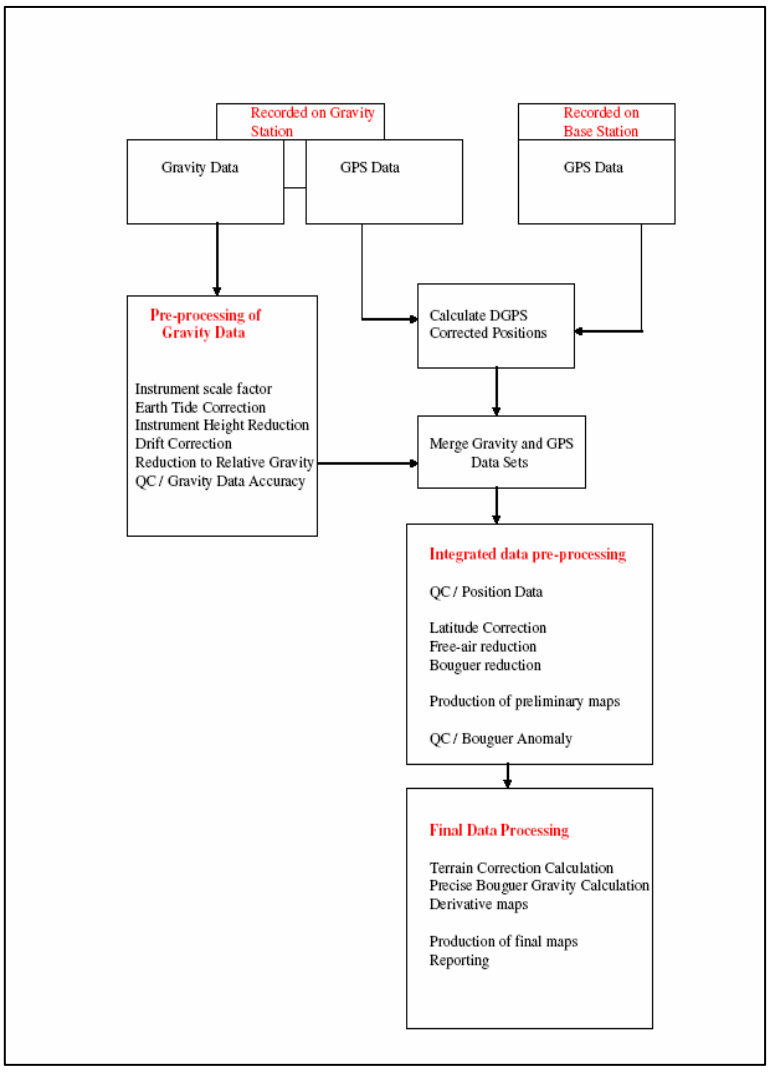

Figure 28: Data Processing Flow Chart – Gravity Survey

The pre-processing or infield processing sequence for the airborne magnetic and radiometric survey included the following quality control measures:

a) Examination and checking of all incoming data to ensure completeness of data sets.
b) The production of preliminary flight path maps, speed checks, terrain clearance checks.
c) Full profile quality control of all acquired traces for noise levels, data completeness, spike editing, and adherence to contract specifications.

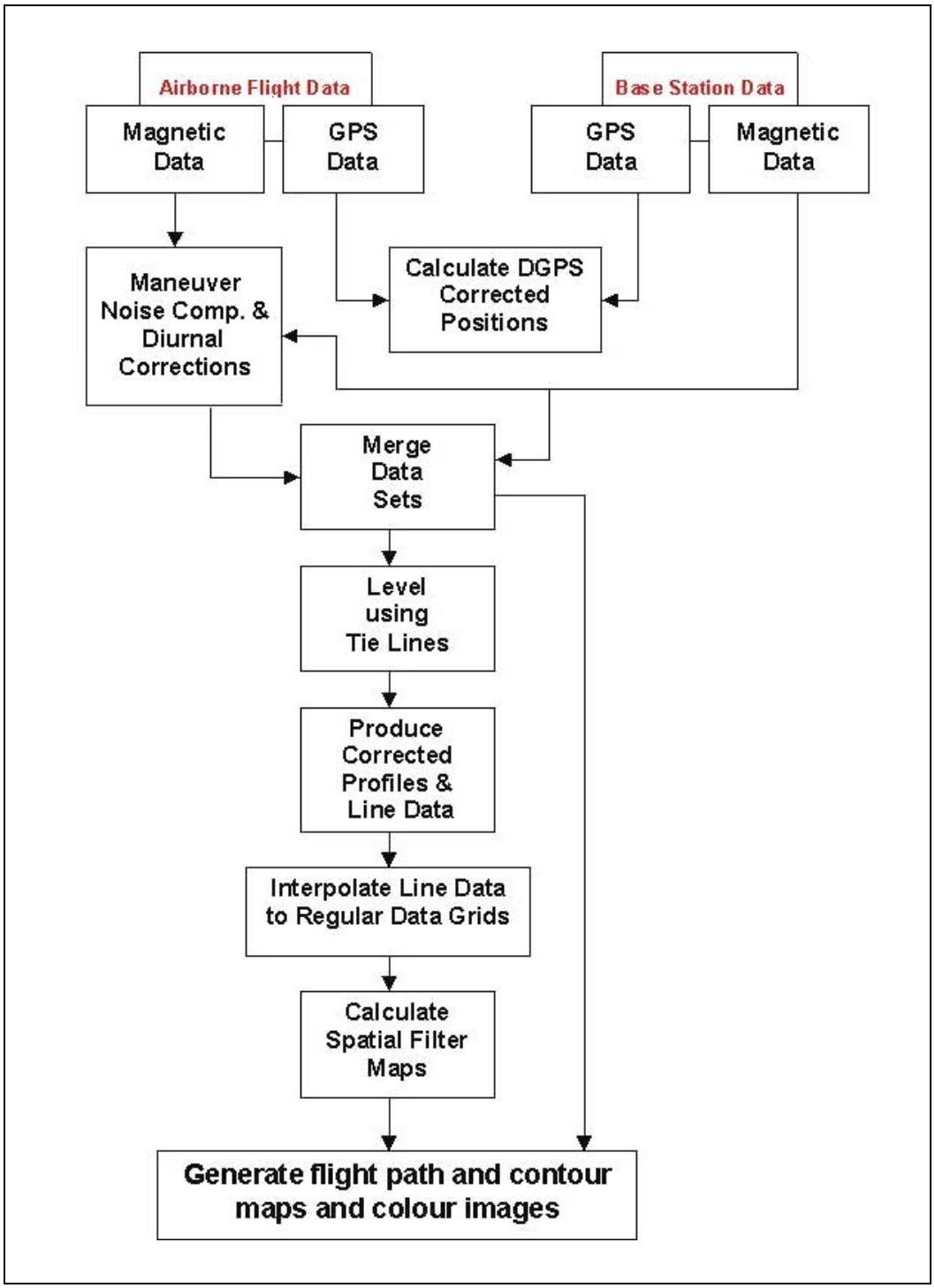

Figure 29: Data Processing Flow Chart – Airborne Magnetic and Radiometric Survey

The final magnetic and radiometric data processing, map generation and report was completed by McPhar at the Newmarket, Ontario office.

7.1 Gravity Survey Data Quality Control

Data quality control included the following procedures:

- Quality Control of gravity data accuracy
- Quality Control of gravity station locations
- Quality Control of GPS data quality
- Quality Control of Bouguer Anomaly Accuracy

7.1.1 Quality Control of Gravity Data Accuracy

Gravity data accuracy was controlled by making repeat readings on selected stations within the survey grid using the following methodology:

1. Using the same gravity meter in an independent loop on more than one day.
2. Using two gravity meters in an independent loop on the same day
3. Using the same gravity meter in the same loop on the same day.

Up to five (5) repeat readings were completed at the same gravity station location. Each repeat reading was evaluated as an individual repeat station.

An overview of the repeat station accuracies is included as Table 20:

Table 20: Overview of Gravity Measurement Accuracies for Individual Blocks

Block	Number of Gravity Stations	Number of Repeat Gravity Readings	Percentage of Repeat Stations in Block	Average Accuracy (mGal)
A	63	4	6.35%	0.012
B	100	6	6.00%	0.025
C	63	10	15.87%	0.012
D	238	12	5.04%	0.019
E	75	6	8.00%	0.008
PROJECT	**539**	**38**	**7.05 %**	**0.024**

A table reporting the gravity accuracies of the repeat stations is included in Appendix 2.

The gravity values recorded during the gravity survey have an accuracy of +/- 0.024 mGal, better than the contract requirement of an accuracy of +/- 0.03 mGal and equivalent to the average of the Standard Deviation of the repeat readings. A total of 38 gravity readings, 7.05% of the total stations surveyed, were completed at 37 individual stations.

The average accuracy of 0.024 mGal includes the cumulative effect of equipment accuracy, seismicity and loop closure error which is typically 0.075 mGal for ground gravity surveys of this type.

7.1.2 Quality Control of Gravity Station Locations

A review of the quality of the location of the gravity stations on Waseco Project is summarised in Table 21 below.

Not all gravity stations could be surveyed within the radius of 60 m from the ideal grid station location because of difficult access (thick bush and/or forest, lake, muskeg and/or poor satellite coverage). All stations that were located outside of the 60m radius from the ideal location were reported by the operator. A detailed list of stations surveyed outside of 60 m radius limit is included in Appendix 2.

In summary, a total of 7.8 % of the gravity stations were relocated outside of the 60 m radius from the ideal grid station location. Quality of the Bouguer Anomaly map was not affected.

Table 21: An Overview of the Quality of the Gravity Station Locations

Distance from ideal planned gravity station location	Number of gravity stations	Percentage of gravity stations
Within of radius 60 m	497	92.2 %
60 m - 75 m	18	3.3 %
75 m – 100 m	21	3.9 %
100 m – 140 m	3	0.6 %

7.1.3 Quality Control of GPS Data Quality and Bouguer Anomaly Accuracy

GPS data quality was controlled by:

- Ensuring that all GPS measurements have a base line distance of no greater than 10km to a GPS Base Station
- Ensuring that a minimum of 6 -8 satellites were always in view when making GPS measurements.
- Automatically by software processing. This process separated the quality of the GPS signals into three categories :

  1. – very good quality – FIXED solution
  2. – good quality – FLOAT solution
  3. – bad quality – NAVIG solution only

All station positions determined by TOPCON Tools as FLOAT or less quality were resurveyed to receive FIXED solution quality designation.

The GPS quality was also controlled by the SD/Accuracy of each solution for X, Y and Z, in millimetres. The average accuracy in Z-component was +/- 2.5 cm, the maximum allowed by the contract was +/- 5 cm.

The accuracy of the X and Y positioning has a minimal effect on the quality of the gravity observation.

The Z component is critical in gravity surveying; the quality of this measurement can be obtained through use of the Standard Deviation of the Z component (SDZ).

The SD/Accuracy of the Bouguer Anomaly was calculated for each gravity station in the following manner:

$$SDBA = SDG + (0.30859 \times SDZ) + (0.0419 \times BD \times SDZ)$$

where:

SDBA is the Standard Deviation /Accuracy of the Bouguer Anomaly,
SDG is the Average SD for the observed gravity value of 0.024 mGal as determined from the repeat stations,
SDZ is the Standard Deviation / Accuracy of the surveyed Z-component as determined from TOPCON software,
BD is the Bouguer Density (values used are either 2.63 gm/cm^3 or 2.80 gm/cm^3 dependent on survey block).

The average accuracy of the Bouguer Anomaly was calculated as 0.035 mGal.

7.2 Preliminary Gravity Data Processing

Preliminary processing of the acquired gravity data was comprised of the following three steps:

- Processing of the raw gravity data
- Processing of the raw GPS data
- Integrated processing of GPS and gravity data

7.2.1 Processing of the Gravity Data

The gravity data was processed using pre-programmed scripts and procedures in GEOSOFT OASIS/ Montaj software.

Pre-processing of gravity data included the following reductions and corrections:

7.2.1.1 Instrument Scale Factor

The instrument scale factor corrects a gravity observation to a relative milliGal (mGal) value based on the instrument dial calibration as supplied by the instrument manufacturer. The correction can be constant throughout the instrument range, or it can be derived from a manufacturer supplied calibration table. The scale factor is applied to the gravity observation as follows:

$$r_c = r \times S(r) \qquad (1)$$

where:

r_c is the corrected reading in milliGals,

r is the instrument reading in dial units and
$S(r)$ is the scale factor (dial units/milliGal), which may be a function of the reading.

For gravity meters L&R G1011 and D108 the original scale factors provided by manufacturer were used and are provided in Appendix 3.

7.2.1.2 Tide Correction

All gravity observations were corrected for Earth tidal effects calculated based on the position of the sun and the moon at the time and location of the gravity observation using the following equation:

$$r_t = r_c + g_{tide} \qquad (2)$$

where:

r_t is the tide corrected reading,
r_c is the scale corrected reading from (1) and
g_{tide} is the tide correction.

The Earth tide corrections were calculated using proprietary software based on the Longman 1959 Formula for Earth tides. Earth tidal values were calculated for a central point common to all survey blocks using the following parameters:

Table 22: Earth Tide Calculation Location

	Longitude	Latitude	GMT
WASECO Project	69.00 W	56.30 N	+5 hours

7.2.1.3 Instrument Height Reduction

Each reading was corrected for the height of the instrument above the station. The instrument height was measured from the bottom of the tripod base plate on which the levelled instrument levelled to the ground. Gravity observations were corrected using the following formula:

$$r_h = r_t + (0.308596)h_I \qquad (3)$$

where:

r_h is the instrument height corrected reading,
r_t is the tide corrected reading from equation (2) and
h_I is the instrument height in metres.

7.2.1.4 Drift Correction Calculation

The gravity meter drift was calculated based on the difference between the first and last base station reading in each daily loop for each individual meter using the following formula:

$$d = \frac{r_{B2} - r_{B1}}{t_{B2} - t_{B1}} \qquad (4)$$

where:

d is the drift in milliGals/hour,
r_{B1} is the reading obtained at base station 1,
t_{B1} is the time of the base station 1 reading,
r_{B2} is the reading obtained at base station 2 and
t_{B2} is the time of the base station 2 reading.

The base station loop closure time period was between 4 to 5 hours.

7.2.1.5 Absolute Gravity Calculation

The absolute gravity is the Earth's gravitational attraction at the gravity observation station calculated using the following formula:

$$g_a = g_{B1} + (r_h - r_{B1}) - (t - t_{B1})d \qquad (5)$$

where:

g_a is the absolute gravity in milliGals,
g_{B1} is the absolute gravity at base station 1 in milliGals,
r_h is the instrument height corrected station reading from (3),
r_{B1} is the reading obtained at base station 1,
t is the time of the reading,
t_{B1} is the time of the base station 1 reading and
d is the drift calculated from (4) in units of milliGals/hour.

For the entire survey, the Gravity Base Station BS 900 was used, with a fixed relative gravity value of 980,000.000 mGal.

The output of absolute gravity was then incorporated into a master gravity database containing the following additional information:

- GPS location of reading
- Gravity station number (St #)
- Type of gravity reading (Flag (1 - repeat station, * – regular station))

- Date of survey
- Time of reading
- Operator #
- Gravity meter #
- Relative gravity value as calculated from equation (5)

7.2.1.6 Processing of GPS Data

The GPS data acquired at the gravity observation station was processed using the TOPCON Tools GPS post-processing software.

The output of GPS data processing was incorporated into the master gravity database:

- Gravity station number (St #)
- Longitude (degrees)
- Latitude (degrees)
- Ellipsoidal height (metres)

A description of the TOPCON Tools GPS Post-processing software can be found at www.topcon.com.

7.2.2 Integrated Processing of GPS and Gravity Data

The GPS and gravity data were merged into a single GEOSOFT database and processed to produce the Bouguer gravity anomaly map and derivative products. The data was processed using GEOSOFT OASIS/Montaj software with pre-programmed scripts and stock procedures.

The following corrections and reductions were applied to the gravity and GPS database.

7.2.2.1 Latitude Correction

The latitude correction requires the theoretical gravity calculated at the gravity observation station location on the earth's spheroid. The 1980 formula for the calculation of the latitude correction was applied to the observed gravity data:

$$g_l = 978032.7 - [1+0.0053024\ sin^2(l)-0.0000058\ sin^2(2l)] \qquad (6)$$

where:

g_l is the theoretical gravity in milliGals (latitude correction) and
l is the latitude of the gravity observation station in degrees.

7.2.2.2 Free Air Anomaly

The free air correction was calculated by subtracting the latitude correction (theoretical gravity) from the relative gravity and adding a correction for the station elevation:

$$g_{fa} = g_a - g_l + 0.308596\, h_s \qquad (7)$$

where:

g_{fa} is the free air anomaly in milliGals,
g_a is the *relative* gravity from equation (5),
g_l is the latitude correction from equation (6) and
h_s is the GPS station elevation in metres (ellipsoidal height).

7.2.2.3 Bouguer Anomaly Calculation

The Bouguer anomaly calculation applies a correction to the free air anomaly for the mass of rock that exists between the station elevation and the spheroid:

$$g_{ba} = g_{fa} - 0.0419088 - [\rho h_s] \qquad (8)$$

where:

g_{ba} is the Bouguer anomaly in milliGals,
g_{fa} is the free air anomaly from equation (7),
ρ is the Bouguer density of the rock in g/cm^3 (values of 2.45 g/cm^3, 2.67 g/cm^3 and 2.80 g/cm^3 were used) and
h_s is the GPS station elevation in metres (ellipsoidal height).

7.3 Final Gravity Data Processing

The final gravity data processing was composed of three major steps:

- Calculation and application of gravity terrain corrections,
- Calculation and preparation of Bouguer Anomaly Maps and Complete Bouguer Anomaly Maps and
- Calculation and preparation of derivative anomaly maps.

7.3.1 Calculation of Gravity Terrain Corrections

The calculation of the gravity terrain corrections consisted of two main steps:

- Preparation of Digital Terrain Model grids and
- Calculation of Terrain Corrections

For the calculation of the gravity terrain corrections a set of digital elevation grids was produced using

the Space Shuttle Radar Thematic Mapper (SRTM) elevation data set for an area significantly larger than the survey blocks.

Gravity terrain corrections are typically calculated for the effect of topography on a Bouguer Anomaly value for all deviations of topography from the gravity station elevation over a distance of 5 m (inner circle) to 168 km (outer circle). The methodology used is to use an ever expanding Terrain corrections were calculated to a distance of 168 km from the gravity station, corresponding to Bible Zone M.

Terrain corrections as applied were calculated using a combination of the method described by Nagy (1966) and that of Kane (1962). To calculate the terrain corrections, the DEM data is "sampled" to a grid mesh centred on the station for which the terrain calculation is to be applied. The correction is calculated based on near zone, intermediate zone and far zone contributions. In the near zone (0 to 1 cells from the station), the algorithm sums the effects of four sloping triangular sections, that describe a surface between the gravity station and the elevation at each diagonal corner. In the intermediate zone (1 to 8 cells), the terrain effect was calculated for each point using the flat topped square prism approach of Nagy (1966). In the far zone, (greater than 8 cells), the terrain effect was derived based on the annular ring segment approximation to a square prism as described by Kane (1962). For more processing efficiency, the far zone calculation can be optimized by de-sampling the outer zone to a coarser averaged grid (i.e. by enlarging the size of each ring segment to 2x2 cells beyond 8 cells, and to 4x4 cells beyond 16 cells, and so on).

When calculating the regional correction, the gravity stations are assumed to lie on a surface defined by the DEM. If the actual gravity stations deviate significantly from this surface, the regional component of the terrain correction will be in error. In the case of the current study, this was not a concern given the low level of topographic deviation, the quality of the DTM used, and the high degree of correlation between the GPS station elevation and DTM elevation.

The Terrain Correction (TC) calculation as applied to this study was comprised of four steps:

- TC calculation for Inner Zone - component T1 – (radius 0 to 250 m) (DTM grid of cell size 20 m x 20 m)
- TC calculation for Central Zone - component T2 – (radius 250 m to 5.24 km) (DTM grid of cell size 50 m x 50 m)
- TC calculation for Outer Zone - component T31 – (radius 5.24 km to 28.87 km) (DTM grid cell size of 250 m x 250 m)
- TC calculation for Outer Zone - component T32 – (radius 28.8 km to 166.7 km) (DTM grid cell size of 1 km x 1 km)

The total TC comprises of three components called T1, T2, T3, as follows:

$$TC = T1 + T2 + T31 + T32 \quad (9)$$

The total TC and its components were calculated with an appropriate unit density.

A spherical Earth model was used for the calculation of the T31 and T32 terrain correction components. A flat Earth model is used for the calculation of the T1 and T2 terrain correction components.

7.3.2 Processing of the Bouguer Anomaly and the Complete Bouguer Anomaly

The following formula for the calculation of the complete Bouguer anomaly was applied to each gravity observation with defined coordinates and a given Bouguer density (g/cm^3) of the rocks ρ.

$$\Delta g_B(\varphi, \lambda, h) = g(\varphi, \lambda, h) - g_n(\varphi) + R_F(\varphi, h) - \delta g_{sf}(h, \rho) + T(\varphi, \lambda, h, \rho) + \delta g_{atm}(h) \qquad (10)$$

where;

$\Delta g_B(\varphi, \lambda, h)$ is the Complete Bouguer Anomaly at a given latitude φ in WGS84 degrees, a given longitude λ in WGS84 degrees, and a given height above the Bouguer geoidal surface h in metres;

$g(\varphi, \lambda, h)$ is the absolute gravity value measured and processed for each station at a given latitude, longitude and height.

$g_n(\varphi)$ is the standard gravity field (latitude correction), calculated using the Somigliani formula where:

$$g_n(\varphi) = \frac{a\gamma_E \cos^2\varphi + c\gamma_P \sin^2\varphi}{\sqrt{a^2\cos^2\varphi + c^2\sin^2\varphi}} \qquad (11)$$

where:

- a is the semi major axis of the WGS84 ellipsoid;
- c is the semi minor axis of the WGS84 ellipsoid;
- γ_E is the calculated standard gravity at the equator for the WGS84 ellipsoid;
- γ_P is the calculated standard gravity at the pole for the WGS84 ellipsoid.

$R_F(\varphi, h)$ is the Free-air reduction for the gravity station at geoidal altitude (h) using Taylor's series of the second order defined by Wenzel, 1985, in Torge, 1989 where:

$$R_F(\varphi, h) = \left.\frac{\partial\gamma}{\partial h}\right|_{h=0} h + \frac{1}{2}\left.\frac{\partial^2\gamma}{\partial h^2}\right|_{h=0} h^2 \qquad (12)$$

and

$$\left.\frac{\partial\gamma}{\partial h}\right|_{h=0} = -\frac{2g_n(\varphi)}{a}\left(1 + f - 2f\sin^2\varphi + \frac{3}{2}f^2 - 2f^2\sin^2\varphi + \frac{1}{2}f^2\sin^4\varphi\right) - 2\omega^2 \qquad (13)$$

and

$$\left.\frac{\partial^2\gamma}{\partial h^2}\right|_{h=0} = \frac{6\gamma_0}{a^2\left(1 - f\sin^2\varphi\right)^2} \qquad (14)$$

where:

$f = (a - c)/a$ is the inverse flattening of the ellipsoid WGS84;

ω is the angular velocity of the Earth.

$\delta g_{sf}(h, \rho)$ is the Bouguer reduction calculated for the gravity effect of a spherical slab with a radius of 166.7 km. This was calculated for each station location using the formula of Cassinis-Dore-Balarin (1937). This is equivalent to calculating the Bouguer reduction using an unlimited horizontal slap corrected by Bullard's term for a spherical shape with a radius of 166.7 km.

$T(\varphi, \lambda, h)$ is the terrain correction calculated to a distance of 166.7 km from each gravity station as defined by equation (9).

$\delta g_{atm}(h)$ is the atmospheric correction as defined by Wenzel (1985), in Torge, 1989 using the density model of the atmosphere defined by:

$$\delta g_{atm}(h) = 8.74 - 9.9 \cdot 10^{-4}\, h + 3.56 \cdot 10^{-8}\, h^{-2} \qquad (15)$$

where $0\ m \leq h \leq 8000\ m$.

7.3.3 WGS84 Ellipsoid Constants

The following constants of the WGS84 ellipsoid were used in all applicable calculations:

$a = 6378137$ m (semi major axis)
$c = 6356752.3$ m (semi minor axis)
$\gamma_E = 9.7803268\ m \cdot s^{-2}$ (standard gravity at equator)
$\gamma_P = 9.8321864\ m \cdot s^{-2}$ (standard gravity at pole)
$\omega = 7.292115 \cdot 10^{-5}\ rad \cdot s^{-1}$ (angular velocity of the Earth)
$f = 0.003352811$ (ellipsoid flattening)

7.3.4 Determination of the Bouguer Density

The Bouguer density ρ of the rocks was determined using Nettleton profile method. This method requires that the Bouguer gravity be calculated for a series of Bouguer densities for gravity observations obtained over a discrete topographic feature (i.e. hill) local to the survey area. The Bouguer density corresponding to the profile which displayed the least correlation to the topography (from both a positive and anti-gravity perspective) is then assumed to be the Bouguer density for the survey grid.

The profiles selected for Nettleton Bouguer density determination were:

- Block II - Profile A - EW direction - from gravity station #5037 to gravity station #5042;
- Block III - Profile A - gravity station #1011 - #1019 - #1029 - #1040 - #1046 - #1055;

- Block IV - Profile A - EW direction - from gravity station #2006 to gravity station #2106;
- Block IV - Profile B - NW direction - from gravity station #2067 to gravity station #2071
- Block V - Profile A - gravity station #3005 - #3014- #3023 - #3041 - #3050 - #3059 - #3068

The Nettleton analysis yielded the following results for the Bouguer density:

Table 23: Bouguer Densities used for each survey block as derived from Nettleton profiles

Survey Block	Bouguer Density (g/cm^3)
I	2.80
II	2.80
III	2.45
IV	2.45
V	2.45

7.3.5 Gridding

The corrected Bouguer anomaly gravity data was interpolated between the gravity survey stations using a random point minimum curvature gridding algorithm to yield x-y grid values for a standard grid cell size of $1/5^{th}$ of the station spacing (100 m).

7.3.6 Filter Derivatives

The Complete Bouguer Anomaly (CBA) data were subjected to:

- Calculation of the First Vertical Derivative (1VD)
- Calculation of the Second Vertical Derivative (2VD)
- Calculation of the Total Horizontal Derivative (TOTHDRV)
- Calculation of the Analytic Signal

Colour/contour images were produced for all the above listed gravity products.

All of these spatial filtering techniques were completed using the GEOSOFT OASIS/Montaj Magmap module for filtering in the 2D FFT domain.

7.3.7 First Vertical Derivative

Vertical derivatives compute the rate of change of the potential field as it drops off when measured vertically over the same point (upward continuation). Potential field data obeys Laplace's equation, which allows for the computation, through the FFT package, to take advantage of this symmetry and solve for the vertical or "z" component of the field. The First Vertical Derivative (1VD) has the effect of sharpening anomalies, which allows for better spatial location of source axes and boundaries.

The First Vertical Derivative was calculated from the Complete Bouguer Anomaly grid.

7.4 Airborne Survey Flight Path Compilation

The airborne survey flight path was derived from differentially corrected GPS positions using the real-time airborne GPS data. A position was calculated every 1.0 second (approx. every 30 meters along the flight path) to an accuracy of better than +/- 1.5 meter. The position data was then merged into the magnetic and radiometric data in the respective Geosoft GDB database.

As part of the QA/QC process, the following GPS parameters were checked on a daily basis:

- Number of satellites under observation (average of 6, minimum of 4 allowed)
- PDOP (position dilution of precision; maximum value of 3 allowed)
- Flight path deviation in X, Y and Z (maximum deviation in X and Y of 50% of line spacing over a linear distance of 5000 metres)

If the above specifications were not met, a reflight was necessary.

All positional data was maintained in WGS 84 (World) coordinates.

7.5 Base Station Magnetic Data

The base station magnetometer data was edited, plotted and merged into the GDB database on a daily basis.

The QA/QC procedure to determine acceptable magnetic base station data involved:

- Despiking of the base station data resulting from cultural activities not associated with the performance of the survey.
- Determination of the maximum noise of the observed total magnetic intensity (TMI; 1 nT maximum allowable).
- Determination of the average 4^{th} difference noise of the signal (maximum of 0.2 nT allowable)
- Determination of the rate of diurnal change (maximum gradient of 4 nT for a 5 minute chord).

7.6 Corrections to the Magnetic Data

The processing of the data involved the application of the following corrections:

- Correction for diurnal variation using the digitally recorded ground base station magnetic values.
- Adjustment of the data for the time lag between the GPS position and the position of the magnetic sensor.
- Correction for the heading effect and

- Network adjustment using the flight line and tie line information to level the survey data set.

The corrected data was then used to generate the Total Magnetic Intensity grid.

7.6.1 Additional Corrections Applied to Profile Data

After applying the above corrections to the magnetic profile data, residual line-direction-related noise was removed through application of microlevelling. The microlevelling technique consists of applying directional and high pass filters to produce a grid containing noise-only in the line direction. In order to differentiate between the two of them, the grid is extracted to the profile database, and an amplitude limit and a filter length are determined, so that the final error channel reflects only noise present on the grid without removing or changing geological signal. This error channel is then subtracted from the initial data channel in order to obtain the final microlevelled channel. The resulting grid is free of line direction noise.

7.6.2 Gridding

The corrected magnetic line data was interpolated between survey lines using a random point minimum curvature gridding algorithm to yield x-y grid values for a standard grid cell size of 1/5th of the line spacing (20 m).

7.6.3 Filter Derivatives

The Total Magnetic Intensity (TMI) data were subjected to:

- IGRF removal
- Reduction-to-the-pole
- Calculation of the First Vertical Derivative (1VD)
- Calculation of the Second Vertical Derivative (2VD)
- Calculation of the Total Horizontal Derivative (TOTHDRV)
- Calculation of the Analytic Signal

Colour/contour images were produced for all the above listed magnetic products.

All of these spatial filtering techniques were completed using the Oasis Montaj Magmap and IGRF modules for filtering in the 2D FFT domain.

7.6.3.1 IGRF Removal

The International Geomagnetic Reference Field (IGRF) is a long-wavelength regional magnetic field calculated from permanent magnetic observatory data collected around the world. The IGRF is updated and determined by an international committee of geophysicists every 5 years. Secular variations in the Earth's magnetic field are incorporated into the determination of the IGRF.

Through the removal of the IGRF from the observed Total Magnetic Intensity (TMI), the resulting

residual magnetic intensity allows for more valid modelling of individual near surface anomalies. Additionally, the data can be more easily incorporated into databases of magnetic data acquired in the past or to be acquired in the future.

7.6.3.2 Reduction-to-the-Pole

To compensate for the shift of the true anomaly position over the causative source, due to the magnetic inclination and declination, the magnetic data was recomputed so that magnetic anomalies would appear as if located at the north magnetic pole. The result of this operation is that in theory, the magnetic anomaly is located directly overtop of the causative source. The computation is referred to as "reduction-to-the-pole" (RTP). The reduction-to-the-pole is computed using a FFT (Fast Fourier Transform) operator.

The RTP not only shifts the anomalies to their correct position with respect to the causative magnetic bodies, but assists in the direct correlation and comparison of magnetic anomalies, trends, structural axis, and discontinuities with mapped geologic surface expression.

The RTP was calculated using the following parameters for the survey areas:

Table 24: Pole reduction parameters by survey Block

Block	Geomagnetic Inclination (degrees)	Geomagnetic Declination (degrees)	IGRF Total Magnetic Intensity (nanoTesla)
Block I	77.30° N	-24.50° E	57090
Block II	77.67° N	-25.59° E	57082
Block III	78.03° N	-24.66° E	57417
Block IV	77.72° N	-23.33° E	57468
Block V	77.38° N	-23.58° E	57278

7.6.3.3 Calculation of the First Vertical Derivative (1VD)

Vertical derivatives compute the rate of change of the field as it drops off when measured vertically over the same point (upward continuation). Potential field data obeys Laplace's equation, which allows for the computation, through the FFT package, to take advantage of this symmetry and solve for the vertical or "z" component of the field. The First Vertical Derivative (1VD) has the effect of sharpening anomalies, which allows for better spatial location of source axes and boundaries.

7.6.3.4 Calculation of the Second Vertical Derivative (2VD)

To enhance local anomalies and to outline the edges of anomalous bodies within the data, a Second Vertical Derivative (2VD) is computed. The 2VD is a powerful interpretive tool and that is used to assist in the delineation of causative bodies and to accurately locate changes in the magnetic field gradients. Better definition of discontinuities and their relationship to geology can be gained from the use of this tool. A 2VD will show steep gradients over faults and positive closures over the "up thrown" blocks.

7.6.3.5 Calculation of the Total Horizontal Derivative (TOTHDRV)

To highlight anomalous areas which may be the result of a magnetic source of limited strike length, a Total Horizontal Derivative (TOTHDRV) is computed. The TOTHDRV is a powerful interpretive tool that can accurately define the edges of magnetic features such as dykes and vertical cylindrical geologic units that have sharp, but limited in area, magnetic gradients and geometry. A TOTHDRV will indicate peak gradients along the edges of narrow dykes and a circular, donut shaped anomaly over vertical cylinder sources.

7.6.3.6 Calculation of the Analytic Signal

The analytic signal is the square root of the sum of the squares of the derivatives in the x, y, and z directions:

$$asig = sqrt (dx*dx + dy*dy + dz*dz)$$

where: asig is the Analytic Signal
sqrt is the square root of
dx is the horizontal gradient in the x direction
dy is the horizontal gradient in the y direction
dz is the vertical gradient in the z direction

The analytic signal is useful in locating the edges of magnetic source bodies, particularly where remanence and/or low magnetic latitude complicates interpretation.

7.7 Corrections to Radiometric Data

7.7.1 Background to Corrections and Processing

Gamma-ray spectrometer surveys are utilized for mapping the concentration and distribution of naturally occurring radioelements. The use of an airborne gamma-ray spectrometer allows for the in-situ analysis of radioelement concentrations of naturally occurring Potassium (K), Uranium (U) and Thorium (Th) in the field.

For a geologist, maps showing concentrations of K, U, and Th can be diagnostic in the mapping of rocks and soils which aid in geological mapping, and in the exploration for uranium, gold, tin and tungsten deposits where the primary mineralization process is often related to K metasomatism or alteration.

Radioactivity measurements from an airborne platform are dependent upon the detection of gamma rays produced through radioactive decay of the nuclide to be detected. Only three radioactive elements emit sufficient gamma radiation to be measured by airborne methods. The three major sources are:

- Potassium-40 (^{40}K) which is 0.011% of all potassium
- Daughter products from the ^{238}U decay series,
- Daughter products from the ^{232}Th decay series.

High energy cosmic rays of non-terrestrial origin can be detected by airborne gamma-ray spectrometer surveys. This cosmic radiation interacts with molecules in the atmosphere, the aircraft, and the NaI detectors resulting in the production of high-energy radiation. This radiation is detectable and increases exponentially with height above sea level and it must be compensated for to obtain reliable and repeatable measurements and the detection of terrestrial radiation sources.

The traditional energy windows used to detect gamma ray radiation from K, Th, and U sources have overlapping areas where the energy recorded for a given element contains some contribution from all three radioelements. A correction procedure, known as stripping, is applied to the data to compensate for this spectral overlapping.

The natural gamma ray spectrum over the range of 0 to approximately 3000 keV is resolved by the spectrometer used into 511 channels, each channel ranging from 5 to 6.5 KeV in width. A separate channel records all high-energy radiation above 3000 KeV, the cosmic radiation contribution. Within the defined radioelement windows, the counts recorded are summed over a given time period.

Care must be taken during the acquisition of gamma-ray spectrometer data because the contribution from radon gas and related decay products in the atmosphere can result in misleading count rates. Radon gas can also diffuse from the ground, but only one radon nuclide is the directly related to the Uranium decay series. In order to minimise the impact of radon "contamination", radiometric surveys are not completed during rain ("washes" radon from the air and increases ground concentrations) or fog conditions and for a period of not less than 2 hours after precipitation has finished in order to allow for dispersion of radon gas to normal background levels.

Radiometric surveys have no depth penetration; most radioactive sources are recorded from the upper 1.5 metres of the ground. Radiometric surveys are in effective over water bodies or snow covered areas, the presence of water (in either liquid or solid state) effectively masks the radiation.

Spectrometer data are recorded in counts per second. The instrumentation requires a fraction of a second to process the incoming data – during this time period no counts are recorded. This interval is referred to as "*equipment down time or system dead-time"*. A correction is applied to compensate for this time period.

7.7.2 Processing Applied Using PRAGA 3 Radiometric Processing System

The reduction of radiometric data follows standard processing steps as outlined in the recommendations of IAEA-TECDOC-1363 - Guidelines for radioelement mapping using gamma ray spectrometry data.

The processing of radiometrics data involved:

1. Correction for system dead-time,
2. Background removal,
3. Cosmic correction (Compton scattering correction)
4. Stripping ratios
5. Effective height calculation (correct for pressure/temperature change),
6. Conversion of count rates to ppm values

Note that the terrain clearance correction is limited to 250 metres to prevent unstable amplification of low counts.

The PRAGA 3 (Pico-Envirotec Radiation Air to Ground Algorithm) software package allows for processing of the spectrometer data using three different streams. The data can be processed using the *standard window (ROI) technique* which follows the IAEA standards and is the simplest method for processing natural radiation data; the *fitting technique* utilizing model detector responses which is optimized for man-made or environmental radiation sources; and the *principal component analysis* technique utilizing either the NASVD or MNF algorithm. All three processing methods were applied to the data for evaluation. The *standard window (ROI) technique* was thought to provide the most geological information and is the method used in the data presentation. As a further QA/QC step, the spectrometer data was also processed using the Geosoft Radiometric Processing System which produced similar but slightly more "filtered" presentation when compared to the PRAGA 3 output.

As part of the processing step the digital elevation model (DEM) is calculated by subtracting the radar altimeter reading from the barometric altimeter reading. The barometric altimeter is levelled using the GPS altimeter. The DEM is calculated as a check on the barometers and to provide information on the topography for interpretation of the radiometric data.

Micro levelling of the radiometric data was completed to eliminate and/or reduce streaking on final gridded images of the individual channels.

8. INTERPRETATION

8.1 Regional Geology

The five (5) claim blocks of Waseco Resources Inc. are located in the Labrador Trough metalliferous geological province of Quebec, Canada.

The Labrador Trough is a thrusted fold belt of Paleo Proterozoic age (2,170-2,140 M.A.) sandwiched between the rocks of the Archaean Superior and Churchill Provinces. The Waseco Claim Blocks are located within the Central Labrador Trough and include portions of the Berard, Cambrian, Melezes, Schefferville and Howse Zones. The Zones are separated from each other by either a thrust fault or an erosional unconformity. The composition of the Central Trough includes volcano sedimentary, fluviatile sandstones and conglomerates, flood basalts and diabase and gabbroic intrusives.

The Labrador Trough underwent extensive exploration activity, primarily spearheaded by the Quebec Government in the 1960's and by various mining companies in the late 1970's and early 1980's.

The primary focus of Waseco is uranium exploration in this area; however the presence of copper, gold, silver, lead, zinc, cobalt and possibly kimberlite can not be overlooked. Uranium occurrences in the survey areas consist of both boulder and limited surficial showings. It is assumed that the mobile uranium mineralisation must have been transported up the sedimentary cover sequence via shear zones from the assumed primary, basement deposits hosted in pegmatitic intrusions in the Archaean basement.

Both Athabasca and Olympic Dam type deposits have been suggested for the Labrador Trough uranium deposits. Although these types of deposits are fundamentally different, they do share some significant common elements, primarily:

- The Archaean basement is the primary source of mineralisation,
- Both are multi metallic with respect to uranium mineralisation, primarily carrying copper and gold,
- That the metal-carrying solutions have, for Olympic Dam deposits, filled open spaces in an explosive volcanic diatreme breccia crater and in the case of the Athabasca type deposits, travelled up through a network of fractures, shear zones and cataclastic zones within the basement and the overlying sedimentary cover sequences.

It is important to note that the Labrador Trough should not solely be considered for uranium deposits but also for massive base metal sulphide (MBMS) and precious metal deposits. There is also the possibility of kimberlite and hence diamonds.

The geophysical implication is that the ideal target may have a deep seated gravity anomaly indicative of a primary basement zone which has been faulted / sheared with an associated near surface fault structure and anomalous magnetic and radiometric responses. The magnetic response may also be indicative of a deep seated causative source body onto which the shallow response of a "younger" fault sequence has been imprinted.

8.2 Regional Geophysical Setting

Regional aeromagnetic and ground gravity observation coverage is available from the Geological Survey of Canada (GSC) covering the entire survey area of interest as 2 km x 2 km gridded data set. The aeromagnetic data was collected by the GSC on flight lines oriented east-west with a line separation of 500 m. The gravity observation data was acquired on a station spacing of approximately 10 km to 20 km interval.

Both the magnetic and the gravimetric images (Figure 29 and Figure 30 respectively) illustrate the pronounced north-northwest – south-southeast regional trend of the Central Labrador Trough. This trend is crosscut at intervals by an east-west to east-northeast – west-southwest trend. These appear to be the major deep seated tectonic trends in this portion of the Labrador Trough. Depth to the crystalline basement based on the regional geophysical datasets is limited by the grid cell size or sampling interval, in this case 2 km, limiting the reliable minimum depth to source to 1 km.

In general, the GSC Bouguer Anomaly map is limited in resolution by the separation between the actual gravity measurement points. In this area, the actual GSC gravity coverage is relatively sparse, varying from 10 km to 20 km. As a result the GSC gravity data will tend to produce a "deep" looking dataset where depth estimates shallower than 2.5 km would be rare, and hence only large scale regional trends can reliably be inferred.

Common to all survey blocks is that they are located over areas of magnetic and gravimetric gradient, suggesting that the survey blocks are in locations of faulting and/or major geologic variation.

Survey Blocks I and II are located on the same north-northwest – south-southeast regional magnetic and gravity trend with Block II also being intersected by an east-northeast – west-southwest magnetic only trend. Survey Block III is at the most northerly of the survey areas and is located on the apparent intersection of the dominant north-northwest – south-southeast gravity trend on the western extent of the dominate gravity low on the regional gravity map (Figure 30) and a weaker, narrower, east-west gravity and magnetic trend. Survey Blocks IV and V are situated on the north side of east-west striking magnetic gradients and to the west of a weak regional north-south magnetic trend. The gravity setting is more complex, in that survey Blocks IV and V appear to be the limbs of a chevron shaped (">") gravity structure.

In general, all survey Blocks appear to meet the general model criteria of a deep gravity source, shallower magnetic source, and situated on or near the junction of major basement structural trends which appear to be related to regional tectonic events (faulting and/or folding) of the basement and metasedimentary rock units.

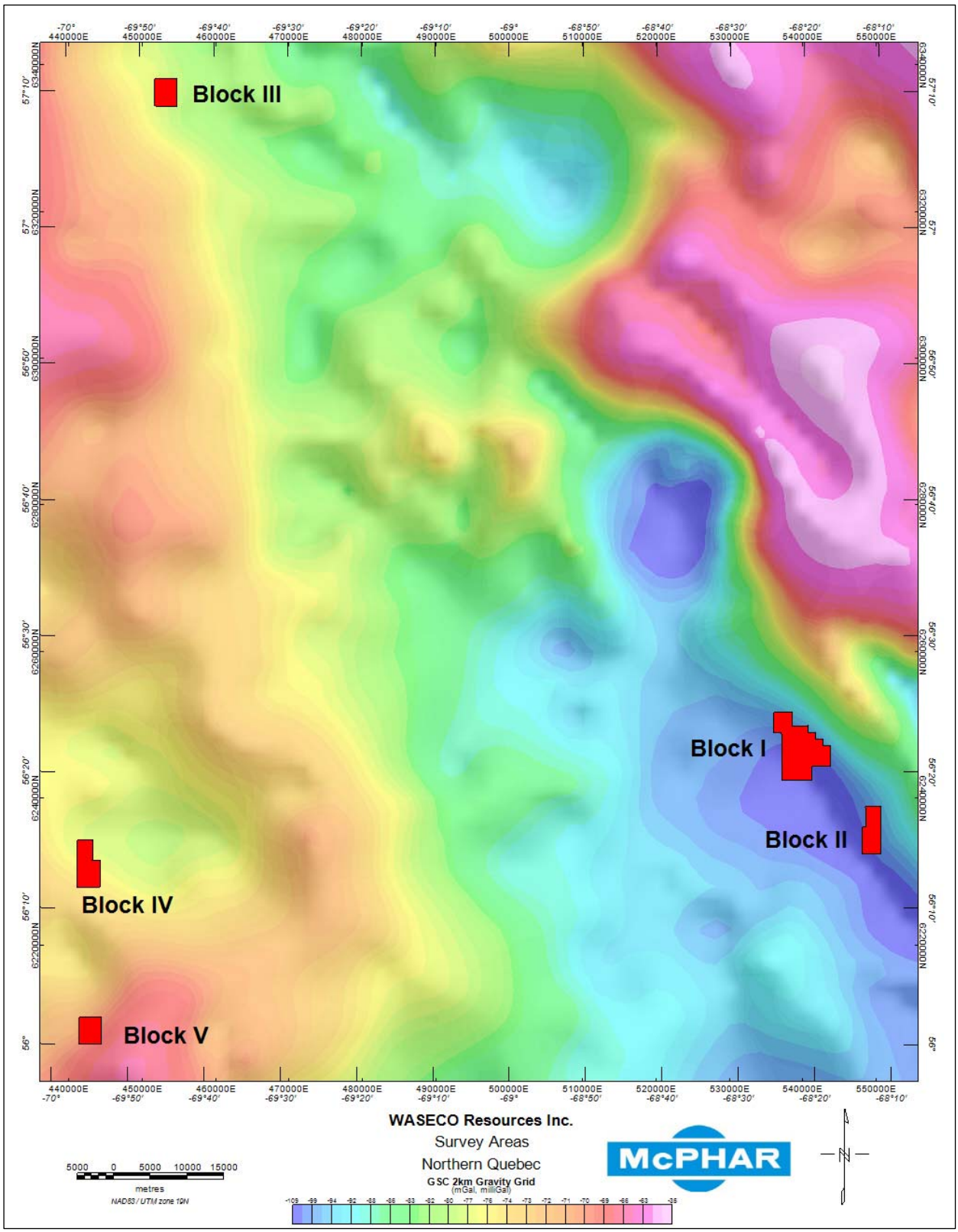

Figure 30: Geological Survey of Canada (GSC) 2 km regional Bouguer gravity grid of the survey areas.

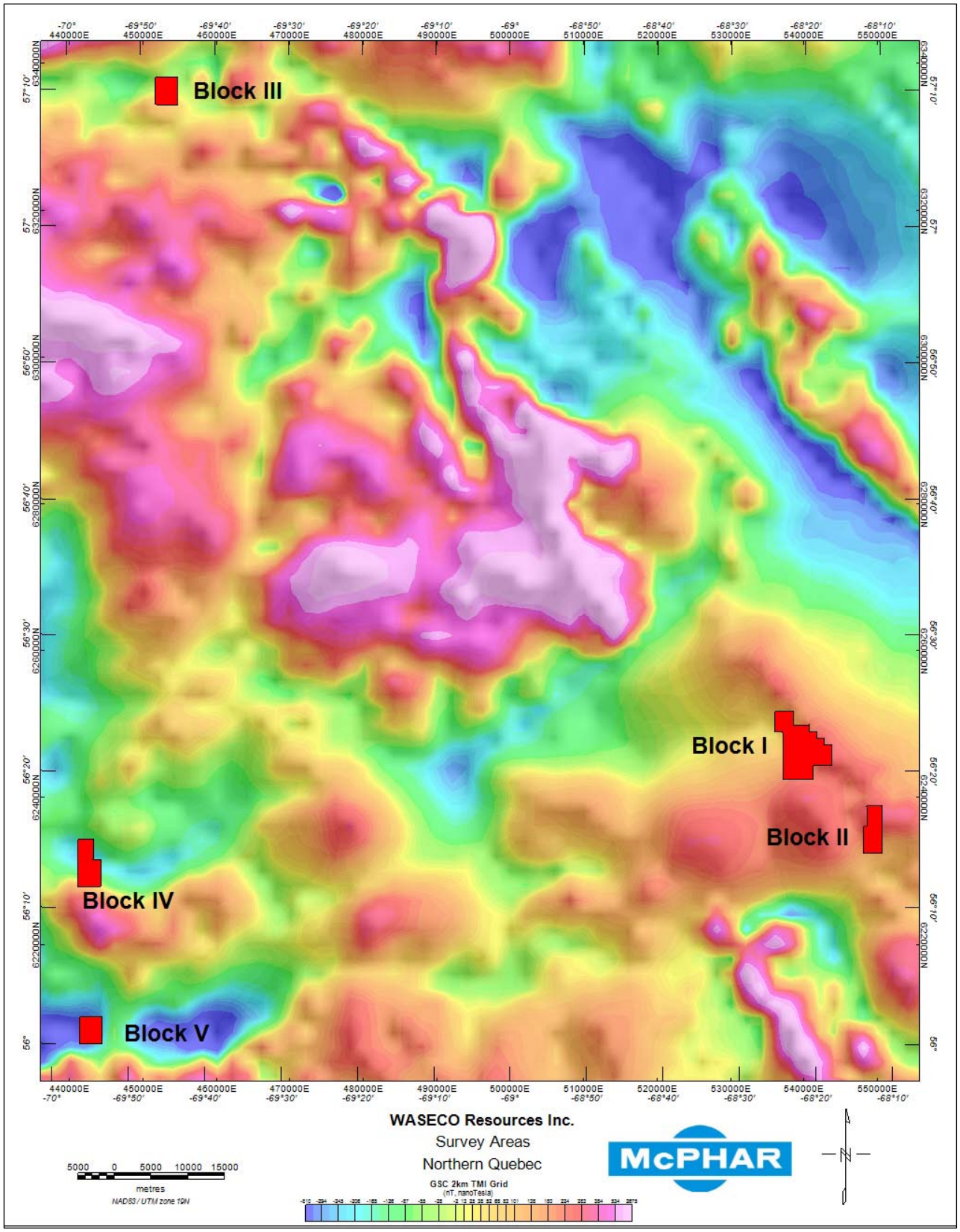

Figure 31. Geological Survey of Canada (GSC) 2 km Total Magnetic Intensity grid of the survey areas.

8.3 Regional Topographic Setting

The regional topography presented in Figure 31 is derived from NASA SRTM 90 data set acquired from the space shuttle radar thematic mapping program and prepared by NASA for the areas covered as a 90 m gridded data set. This data set was compared to the 1:250,000 topographic maps available from Government of Canada. The SRTM 90 data was judged to correlate favourably with the published topographic maps.

The regional topography is dominated by the north-south valley of the Lac Cambrian, Riviere Swampy, Riviere Cataract system which divides the regional area into two halves. The area to the west of Lac Cambrian – Riveire Cataract contains the highest elevations, particularly in the southwest in the vicinity of Survey Blocks IV and V. The area to the east is typically lower and with less relief. To the east of the Riviere Swampy the general topography is flatter; with a series of long narrow ridges striking north-northwest south-southeast that resembles an upturned (on edge) folded sedimentary section. This feature is particularly well developed along the eastern edge of Survey Blocks I and II.

Elevation varies from approximately 60 m above sea level at the extreme north central to over 500 m in the southwest. Drainage is from south to north. If the general trends in the topography can be assumed to indicate the direction of glacier retreat during the most recent ice age, then the glaciers appear to have retreated along the Lac Cambrian – Riveire Cataract. Topographic trends in the west half are north-northeast south-southwest with what may be large terminal moraines striking northwest-southeast in the vicinity of Survey Block III. To the east of the Lac Cambrian – Riveire Cataract valley, the trend is north-northwest south-southeast. Both the east and west topographic half trends converge on the Lac Cambrian – Riveire Cataract valley.

Based on the regional topography, the near station topography will have an effect on the final Bouguer gravity anomaly and terrain corrections are required.

From the airborne magnetic and radiometric survey it is possible to generate an additional DTM for the individual Survey Blocks. This is accomplished through use of the recorded radar altimeter and GPS height data. The accuracy of this calculation is somewhat dependent on the survey conditions and local topography and typically has an absolute error of +/- 2.5 m. The formula for calculating the DTM is:

$$DTM = GPSalt - RADalt$$

where: DTM is the Digital Terrain Model
GPSalt is the height of the aircraft as determined by the global positioning system above the geoid (WGS84) expressed in metres.
RADalt is the height of the aircraft above the ground surface as determined by the radar altimeter, filtered and converted from millivolts to metres.

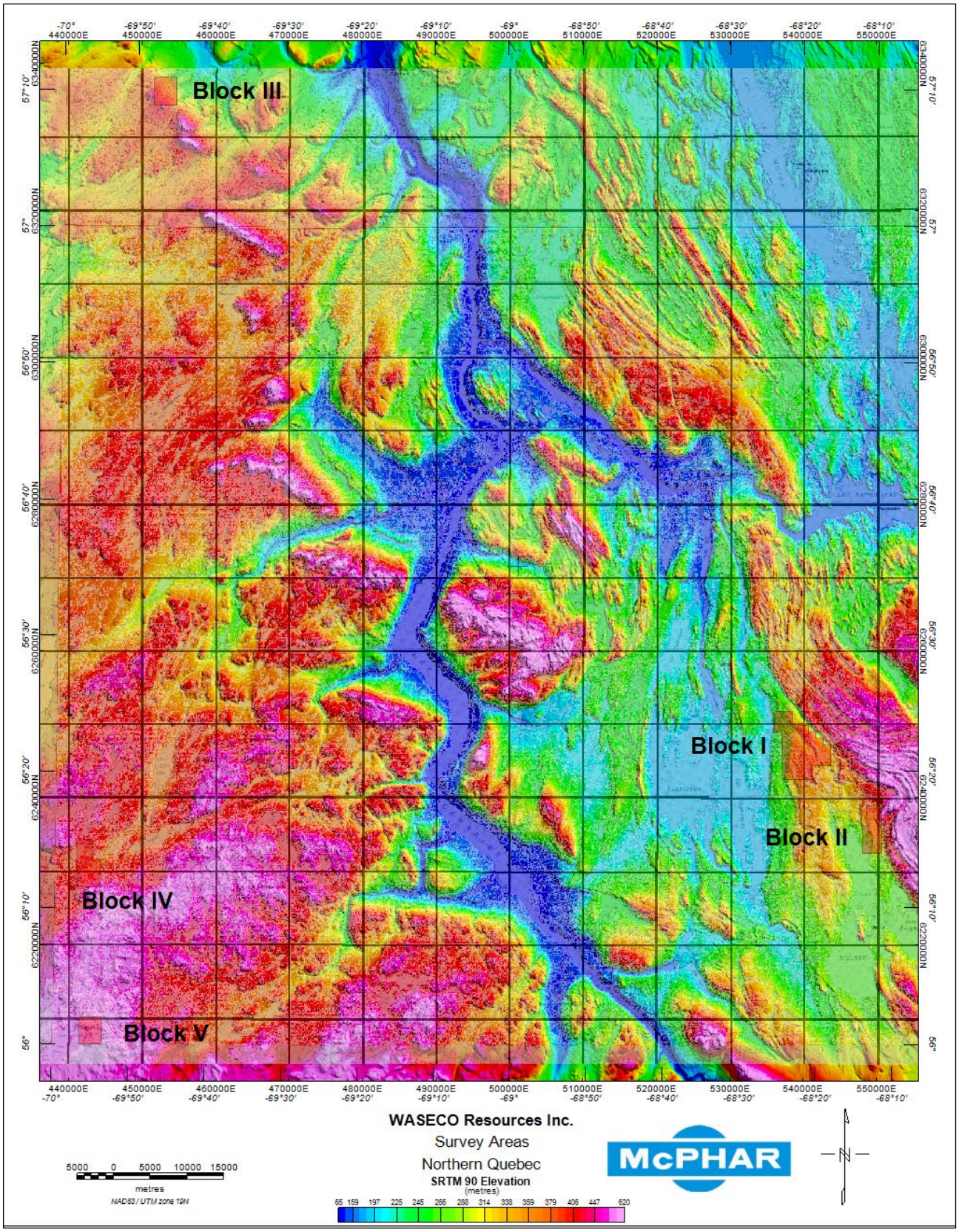

Figure 32: SRTM 90 Elevation DTM with screened 1:250 000 topographic data and Survey Block locations.

8.4 Data Processing for Interpretation

The area covered by the completed multi-discipline geophysical survey is geologically complex. Each Block surveyed contains elements of what geophysically appear to be magnetic dykes, upturned metasedimentary sequences with possible Iron Formations, and thick sections of metasediments, possibly granitic intrusions and other smaller intrusive bodies.

In order to provide a structural interpretation of the area surveyed, the following products were generated and used in the interpretation:

1. All gradient data (TOTHDRV, 1VD, 2VD and Analytic Signal) for both the gravity and magnetic gridded data were calculated and analysed in an attempt to define structural controls on the geology and to identify zones of possible economic mineral resource.
2. Analysis of the individual radioelement data sets (K, U, Th, TC) and the ratio products (U/Th; U/K; Th/K and Ternary) to identify geology and zones of Uranium enrichment.
3. Kimberlite – like intrusive identification has been attempted through the application of "Keating Correlation Coefficient" analysis to the magnetic data.
4. Examination of the magnetic RTP and RTP IGRF Removed maps in conjunction with the gravity CBA maps.
5. Application of Source Parameter Imaging (SPI) in an attempt to define areas of constant magnetisation and provide an estimate of the depth to the magnetic source.
6. Application of Source Edge Detection (SED) to the magnetic and gravity data for each Block to attempt to better define the contacts of the geology through the processing of the magnetic and gravity gridded datasets together.
7. Application of Euler Deconvolution Depth Analysis to both the magnetic and gravity data in an attempt to better define the depth to the causative source bodies.
8. Selected modelling of individual magnetic and gravimetric anomalies.

The following sections briefly describe the processes applied to complete the interpretation.

8.4.1 Total Horizontal Derivative of the TMI and CBA

In order to better define the spatial location of magnetic and gravimetric discontinuities, the horizontal gradient of the TMI-RTP and the CBA was calculated. The *Calculated Horizontal Gradient* was derived using the following procedure:

- The horizontal gradients in the grid x and y directions were calculated from the TMI-RTP and from the CBA gridded data.
- The horizontal gradients were inspected for residual line levelling noise and microlevelled as necessary.

- The vector sum of gradients was computed by calculating the square root of the sum of the squares of the individual gradients using the following equation:

$$\sqrt{\left(\frac{\partial z}{\partial x}\right)^2 + \left(\frac{\partial z}{\partial y}\right)^2}$$

where: $\partial z/\partial x$ *is the rate of change (slope) of the magnetic or gravimetric gradient in the grid x direction*
$\partial z/\partial y$ *is the rate of change (slope) of the magnetic or gravimetric gradient in the grid y direction*

The effect of this process is to sharpen the definition of the edges of the causative bodies from which the geophysical responses are derived.

8.4.2 First Vertical Derivative (1VD) of the TMI and CBA

The vertical derivative is the computation of the rate of change of the magnetic field when measured vertically over a given location. Potential field data obeys Laplace's equation, implying a symmetry at a given location in the vertical or "z" component of the magnetic and gravimetric field.

The net effect of calculating the first vertical derivative (1VD) when applied to the RTP-TMI is the increased definition and/or sharpening of individual anomalies, allowing for better spatial location of magnetic source axes and boundaries, the vertical gradient reaching a maxima directly over the point of inflection in the TMI field, therefore defining the approximate edges of the causative body. In the example of a large, broad magnetic unit, the maxima of the anomaly will generally occur over the centre of the magnetic body with minima over the edge of the body.

When applied to gravimetric data, the calculation of a 1VD is the equivalent of removing a regional long wavelength component from the CBA. The result is the residual response similar to that of the RTP-TMI in that the 1VD maxima will occur over the centre of the gravity anomaly with minima over the edges.

The 1VD is particularly useful in the determination of fault zones and unit boundaries.

8.4.3 Second Vertical Derivative (2VD) of the TMI

Potential field anomalies have inflection points on the anomaly curve related to rock property boundaries. Through the application of the reduced-to the pole operator, the magnetic anomaly over a vertically sided, magnetically susceptible body attains a minimum value over the center of the body, with the steepest gradient (horizontal derivative) occurring over the edge of the body. The anomaly changes from concave to convex at a point where the horizontal derivative of the gradient is zero. If the points where the second horizontal derivative approaches zero can be located, the positions of faults or unit boundaries (magnetic discontinuities) can be inferred.

When attempting to apply this in three dimensions the problem becomes more difficult. As common

practice in geophysical surveying is to plan profiles crossing normal to geologic strike and therefore assuming that the geology is two-dimensional, the second vertical must, to be effective, delineate the edges of the edges of the three-dimensional bodies. To accomplish this, both horizontal components of the potential field being evaluated must be considered as follows:

Laplace's equation as applied to potential fields states:

$$\frac{\partial^2 u}{\partial x^2} + \frac{\partial^2 u}{\partial y^2} + \frac{\partial^2 u}{\partial z^2} = 0 \qquad (1)$$

Rearranging the equation yields:

$$\frac{\partial^2 u}{\partial z^2} = - \left(\frac{\partial^2 u}{\partial x^2} + \frac{\partial^2 u}{\partial y^2} \right) \qquad (2)$$

The implication of this rearrangement is that the second vertical derivative of a potential field is the negative sum of the second horizontal derivatives; therefore the second vertical derivative approaches zero on plan view at the edges of a three-dimensional causative source. The zero (0) contour on a 2VD map will therefore delineate the edges of a causative source.

To apply this methodology to the current magnetic and gravimetric data, the gridded data is Fourier transformed into the frequency domain, then transformed into a second vertical derivative grid using a filter with a response function of:

$$W = 4\pi^2 (f_x^2 + f_y^2)$$

This function is derived from equation (2) where:

f_x^2 = *frequency in the x direction, and*
f_y^2 = *frequency in the y direction*

The second vertical derivative grid in the frequency domain was then inverse Fourier transformed into space domain for presentation.

The result is that the second vertical derivative will show steep gradients over faults and positive closures over the up thrown blocks.

8.4.4 Analytic Signal

The analytic signal method uses the square root of the sum of the squares of the partial derivatives in the x, y, and z directions.

When applied, the analytic signal method generally produces good horizontal locations for contacts and sheet sources regardless of geologic dip or the geomagnetic latitude. Analogous to the horizontal gradient, the analytic signal allows for further refinement and discrimination of magnetic contacts and

source locations.

8.4.5 Source Parameter Imaging

Source Parameter Imaging (SPI) is a procedure for the automatic calculation of magnetic source depths from gridded magnetic data. The procedure was developed by Thurston and Smith (1997) formerly of Geoterrex Limited. The depth solutions calculated are independent of magnetic inclination and declination and therefore do not require that the magnetic data be reduced to the magnetic pole.

The method of calculating the source depth assumes a step-type magnetic and geologic model. The process first calculates the magnetisation (K) and then locates peak K values to compute the depth to the magnetic source.

8.4.6 Euler Deconvolution Depth Estimates

Magnetic interpretations are based on the observed gradients resulting from the presence of magnetic susceptibility boundaries. Gravity interpretations are based on the observed gradients resulting from the presence of density boundaries or contrasts. This implies a juxtaposition of rock with contrasting magnetic and gravimetric characteristics and content which may arise from any combination or all of the following assumptions:

- Lateral variation of magnetic/density content within a lithologic unit, i.e. lateral facies change in a sedimentary unit, heavy sand or gravel deposits in paleo stream channels, varying thickness of an iron rich bed within a shale unit.
- Fault movement resulting in rocks of differing magnetic/density properties being positioned adjacent to each other.
- Fluid migration along fault boundaries or other planes of weakness resulting in the destruction or enrichment through deposition or chemical alteration of the mineralization to more or less magnetic/dense minerals.
- Structural juxtaposition of two or more different lithologies as the result of fold processes.
- Presence of mafic and ultramafic rock units which may penetrate through or crosscut the existing sedimentary lithologic units, i.e. gabbro dykes, plugs and sills, kimberlite pipes.

Analysis of the magnetic and gravity data for depth estimation purposes was achieved through application of 3-D Euler Deconvolution depth estimation as implemented by GEOSOFT. This technique allows for a large amount of data in grid form to be evaluated in a relatively efficient manner. Care must be used in the preparation of the data in order that spurious and erroneous solutions are minimized. The major source of "noise" in the application of Euler deconvolution depth analysis arises from residual line levelling errors and signal aliasing resulting from the gridding method used in the preparation of the gridded data sets.

A significant advantage of the Euler deconvolution method is the inherent insensitivity to magnetic inclination and declination and hence the effects of remanent magnetization when dealing with magnetic data.

Based on Euler's homogeneity equation; an equation relating the potential field (in the case of this study, magnetics) and its' gradient components to the location of a source of a given geometry of homogeneity N, Euler deconvolution depth estimation can be very diagnostic in the location of magnetic faults and causative bodies. The degree of homogeneity N, or *structural index,* is a measure of the rate of change with distance of a potential field and is assumed to be a constant for a given geometry. In application to magnetic data, a narrow 2-D dyke has a structural index of N=1 whereas a vertical pipe-like intrusive body has a structural index of N=2. In application to gravity data, a narrow 2-D dyke has a structural index of N=0 whereas a vertical pipe-like intrusive body has a structural index of N=1.

To solve Euler's equation simultaneously for each position in a gridded dataset, a least squares method is used. A square window is defined in terms of grid cells (in the case of this study, 10 cells by 10 cells) and is passed along each row of gridded data. At each grid point within the window the Euler equation is solved for from which four (4) unknowns (location X, Y, Z and a background potential field value B) and their uncertainties are derived for a given structural index.

A depth solution is recorded if the uncertainty of the calculated depth is less than a specified tolerance (in the case of this study, 15%) and the solution is within a limiting distance of the center of the data window.

In the example of the current study, Euler's homogeneity equation can be stated as follows:

$$(x-x_0)\frac{\partial T}{\partial x} + (y-y_0)\frac{\partial T}{\partial y} + (z-z_0)\frac{\partial T}{\partial z} = N(B-T)$$

where : (x_0, y_0, z_0) is the position of the magnetic/gravity sources,
T is the total magnetic intensity or complete Bouguer Anomaly measured/calculated at (x_0, y_0, z_0),
B is the regional value of the total magnetic intensity or complete Bouguer anomaly, and
N is the degree of homogeneity or structural index

The results of the calculation are then collated and plotted in plan as an Euler "bubble map" with the colour of the "bubble" indicating the depth of the solution. Clustering of solutions will occur along lineaments related to the structural index used in the equation. In the case of the current study, structural indices of 0 (density contacts, gravity only), 1 (narrow dykes, magnetic faults; and gravity pipe or wide bodies) and 2 (line of magnetic dipoles) were applied and the results plotted.

A pseudo depth to basement map was calculated for each set of Euler deconvolution solutions obtained and is presented on the Euler "bubble map".

The Euler Deconvolution depth solutions have also been included as separate GEOSOFT databases and

XYZ files in Appendix 5.

8.4.7 Source Edge Detection

The Source Edge Detection (SED) function is designed such that location of edges (i.e. geologic contacts, faults, etc.) from the analysis of the gradients within the magnetic and gravity data sets.

The technique used is that described by Cordell and Grauch (1982, 1987). A database is constructed which holds the source edge locations as derived from the grid of the total magnetic intensity and complete Bouguer Anomaly. A map is then produced containing geologic strike and dip symbols indicating the gradient directions of the combined gravity and magnetic anomalies. The gradients are grouped based on whether there exist in 1, 2, 3 or 4 directions.

The SED function estimates the location of abrupt lateral changes in magnetization and density of the crustal rock units.

8.4.8 Radiometric Ratios and Ternary Mapping

The apparent concentration of radioelement K, U, and Th channels are often used to produce the standard ratios of U/K, U/Th and Th/K. Through the process of calculating the radioelement ratios, one can often identify subtle variances in the data that may have a significant geological impact with respect to the commodity being explored for.

A Ternary colour plot was used to attempt to present the acquired two dimensional (2-D) radioelement data (K, U, Th) in three dimensions (3-D). The common convention used to produce a ternary plot is to assign a colour to each of the three (3) radioelements. The colour convention used was:

- Uranium (U) – yellow
- Potassium (K) – magenta
- Thorium (Th) – cyan

At each of the vertices of the triangle, the colours are displayed at full intensity without any contribution from the other colours. At the mid point of the side opposite a given vertices, the colour intensity assigned to the vertices is zero (0). At the centre of the ternary triangle, the colour intensity is one-half of each colour resulting in a “grey” or black spot.

The ternary plot is a useful tool in the mapping of geologic units and in the identification of relationships between the three (3) radioelements (U, K, and Th) that can be subtle and of interest.

8.5 Interpretation of Survey Blocks

All Survey Blocks have undergone the same sequence and type of geophysical surveying. The data have all been processed and treated in the same fashion for all areas. The following discussion of the results and the implication of the results have been dealt with on an individual Survey Block basis.

8.5.1 Block I – Lac Bravo, Lac Crabe and Lac du Portage

8.5.1.1 Geology

Situated on the lithotectonic boundary between the Howse zone to the northeast and the Schefferville zone to the southwest; numerous occurrences of uraniferous mineralisation have been documented by previous exploration activity. The Argencourt thrust fault appears to strike through survey Block along the northeast margin of the survey Block.

Past exploration activities by Eldorado Nuclear in 1979 have resulted in the identification of three (3) showings within the survey Block and within the Argencourt fault zone.

The first of these showings, catalogued by the M.E.R.Q. as #181 – Bravo Lake Showing, is characterised by disseminated uraniferous nodules in calcareous dolomites within shear zones comprising the Argencourt fault zone. The mineralisation has also been noted in fractures and cataclastics in addition to shear zones. Numerous trenches occur adjacent to the Bravo showing over a length of 200 m. Glacial boulder trains in the vicinity of the showing have been noted to carry uranium and copper mineralisation. Uranium mineralisation is often accompanied by chalcopyrite, digenite and malachite with minor amounts of gold. Lead, zinc, cobalt, manganese, silver, thorium, vanadium and barium have also been documented. The uranium appears to have been remobilised and can run up to 38% in grab sample.

To the north and west of the Bravo Lake Showing is #185 – Lac Crabe Showing. Hosted within schist with limestone intercalations is disseminated and vein Cu and U mineralisation. This zone extends over 955 m and is up to 1.2 m in width and 45 m in thickness. Previous drilling indicates Cu grades of up to 3.71% over 1.8 m and 0.07% U over 1.2 m.

Strata-bound U in arkosic sandstone comprises showing #187. This is the final showing in the survey Block which is thought to be dominated by the Argencourt fault zone.

Vein U has been observed at showing #188 (Portage Lake Showing) in the southwest of the Survey Block.

8.5.1.2 Gravity

The Complete Bouguer Anomaly (CBA) Map is dominated by a northwest-southeast trending gradient along the northeast edge of the survey block. This feature is interpreted as the gravity response of the Argencourt fault zone. The fault zone is visible on the total horizontal derivative (TOTHdrv) of the CBA as a long linear gradient extending across the survey block with a width of approximately 500 metres. This suggests that the shear zone itself has undergone an increase in

density as a result of the tectonic processes. An offset in the fault zone is visible in the southeast where the strike of the zone changes from northwest-southeast to north-south. The offset is interpreted as a younger fault striking northeast-southwest.

The known U occurrences all flank the gravitational anomaly associated with the Argencourt fault zone. Showings 187 and 188 are on strike or in close proximity to the younger fault which offsets the Argencourt fault zone.

The sharpness of the gravity gradient across the fault zone suggests a large density contrast extending from the surface to depth. The denser material is to be found to the northeast of the fault zone (Howse lithotectonic zone?), the less dense material to the southwest (Schefferville lithotectonic zone?). This type of gravity response may also be indicative of denser intrusive rocks overlain by the less dense sediments to the northeast of the Argencourt fault zone.

Euler deconvolution depth estimates suggest that the main Argencourt fault zone density anomaly is narrow and focussed with depth, ranging from 220 metres to over 600 metres in depth. The Depth solutions, particularly those corresponding to a Structural Index of 0.0 (contact) indicate a sub parallel fault to the northeast that is deeper (500 metres). A possibly older and deep fault is also suggested to the southwest (~1000 metre depth). All currently identified showings fall in areas of diffuse depth solutions that become more focussed with depth, suggestive of the showings and boulder trains being related to the surface expression of deep rooted fault zones. Source Edge Detection (SED) suggests that all faults are dipping to the southwest, suggesting an on echelon series of faults.

8.5.1.3 Magnetics

The Total Magnetic Intensity (TMI) map displays a series of narrow, high amplitude, long linear magnetic anomalies trending northwest-southeast. The two dominant high amplitude linear anomalies correspond to the Argencourt fault zone and flank the gravity density anomaly. To the northeast are sub parallel lower amplitude linear anomalies that appear to be stratigraphic in aspect. A weaker, similar pattern is discernible to the southwest of the Argencourt fault zone.

Vertical derivatives, SPI and analytic signal results suggest that the strata to the southwest of the Argencourt fault are magnetically homogenous with the sedimentary rocks of the lithotectonic Schefferville Zone horizontal. Euler deconvolution solutions based on the magnetic data are shallower in general compared to the gravity data (100 metre versus 500 metres). Mineral showings 181, 185 and 187 all have a shallow magnetic expression and are magnetically part of the Argencourt fault zone.

There are six (6) identified discrete magnetic anomalies that are tight, well defined and generally indicative of a vertical pipe-like intrusive and therefore of possible interest for kimberlite exploration.

8.5.1.4 Radiometrics

The radiometric maps are diagnostic for identifying the near surface geology. In this survey block, the Argencourt fault zone is defined by an absence of radiometric signal along the contact with the Howse lithotectonic zone (footwall) rocks. This low is visible on the Total Count, Potassium and Thorium maps. Faults thought to be of similar age (those sub parallel and to the southwest of the Argencourt fault zone) also exhibit this lack of radiometric activity. It is important to note that these same interpreted faults are also composed of chains of small lakes and rivers. The presence of water can significantly reduce the radiometric count rate and therefore result in "false" radiometric lows. There is very good correlation between the radiometric lows and the bodies of water, however the radiometric lows tend to be significantly larger than the water bodies, indicating either a shallow water table and/or a coincidental depletion of radiometric elements, most likely the result of tectonic activity.

In sharp contrast are the interpreted "younger" faults trending northeast-southwest. This family of faults appears to be enriched in Potassium and Thorium. The hanging-wall or western margin of the Argencourt fault zone is an area of local enrichment in Potassium and Thorium, manifest as a thin (200 m wide) radiometric high along the fault margin.

Thorium and Potassium enrichment also occurs in the area to the immediate north, east and south of showing 187, suggesting that the rocks in this area are of a more intrusive, possibly mafic origin.

Potassium enrichment is also observed in the south central part of the survey block. This is suggestive and consistent with the arkosic metasedimentary unit identified as the host rock for showing 188. The presence of gabbroic dykes in this area is supported by long thin Thorium anomalies crosscutting the metasedimentary sandstones.

Uranium enrichment is prevalent in the northwest of the survey block, centred on showing 185 and extending as far down trend to showing 181. This zone of Uranium enrichment is apparently open to the northwest. There are three (3) Uranium anomalies observed to the northeast of the Argencourt fault zone. These anomalies are within the Howse lithotectonic zone and may be associated with basalt flows, as the Thorium count is also elevated. There are five (5) discrete Uranium anomalies hosted within the Argencourt fault zone or immediately flanking the zone. An additional three (3) Uranium anomalies are hosted within the arkosic sandstone in the western part of the survey area, associated with north-northwest trending faults.

8.5.1.5 Discussion of Results

The general geologic model for this survey block supported by the geophysical surveys is that of a thrust/shear zone comprising the Argencourt fault zone trending northwest near the northeast of the survey area. The fault zone is open to the northwest and southeast. The assumed footwall comprises the Howse lithotectonic zone, with the footwall comprising the Schefferville lithotectonic zone.

Faulting is not restricted to Argencourt fault zone, there are sub parallel and hence possibly contemporaneous in age, faults visible to the northeast and southwest. These faults are less well defined and do not appear to be as continuous as the Argencourt fault zone. A second family of

faults crosscuts the survey block trending northeast – southwest. Both families of faults appear to control the extent and possibly the location of Uranium mineralisation.

The presence of gabbroic (mafic) dykes is supported by both the magnetic and radiometric survey data. The dykes trend northwest and exhibit a moderate enrichment in Thorium with little or no Potassium. Magnetically the dykes are low to moderate amplitude (~200 nT), narrow (<200 m) and up to 3 km in length.

The strongest and most continuous magnetic anomalies are associated with Argencourt fault zone and the Howse lithotectonic zone. The Howse anomalies are interpreted as being stratigraphically controlled and maybe indicative of basalt flows interwoven within the sedimentary sequence. The magnetic anomalies associated with the Argencourt fault tend to occur along the edge of the associated gravity anomaly may be metasediments and /or Iron Formation and hence prospective for gold (Au) and possibly base metal suphides. This is a significant zone that requires further exploration.

There appears to be three (3) distinct types of Uranium target in this survey block. Type 1 targets are hosted in the Howse Zone, Type 2 targets are hosted in or in close proximity to the Argencourt fault zone, and Type 3 targets are hosted in the arkosic sandstone. Common to all Uranium targets is that they are located along interpreted faults.

The Type 1 targets have in common a coincident magnetic response related to local, small scale faults trending northwest. These targets all are hosted within a Thorium enriched, Potassium depleted unit, suggestive of basalt or gabbro host rock.

Type 2 Uranium targets tend to be associated with the west flank of the Argencourt fault zone. The amplitude of these anomalies is greater than the others, typically 4^{+} ppm. Showings 181 and185 are examples of what may be encountered with these Uranium anomalies.

Type 3 Uranium targets are hosted by the interpreted arkosic sandstone sequence in the south and west of the survey block. These targets may reflect an Athabasca Basin type of deposit. These targets are thought to be contemporaneous in age or very slightly older than the Type 2 targets.

A total of six (6) discrete, pipe-like (vertical cylinder), dipolar magnetic responses have been identified. These targets are primarily hosted by rocks comprising the Schefferville lithotectonic zone and at the intersection of the two identified fault families.

8.5.1.6 Recommendations

A total of twelve (12) Uranium and seven (7) magnetic anomalies have been identified as requiring further study. In addition, the original reported showings 181, 185, 187 and 188 should be re-evaluated. In particular the area to the north and west of showings 185 and 181 to the edge of the current claim block should be mapped and explored for uraniferous mineralization as this area exhibits elevated Uranium values.

The entire survey block is considered high priority for follow-up and hence has not been subdivided

into smaller detail areas. In particular the Argencourt fault zone is the most prospective for Uranium mineralisation, particularly on trend to the northwest as the overall Uranium response is anomalous in this area.

The seven (7) magnetic anomalies are anomalous in that they are at or near-surface and are consistent with a vertical pipe-like intrusion and hence may be kimberlitic in origin.

It is strongly suggested that future exploration efforts in this block include heavy mineral sampling in the immediate area around the identified magnetic pipe-like intrusives for kimberlite indicator minerals and diamond. Geochemical sampling of the residual soils and lake sediment sampling for Uranium enrichment accompanied by detailed geologic mapping is required to effectively tie in the reported showings and the current geophysical survey data.

Ground geophysical surveying using either Induced Polarisation (IP) or Time Domain ElectroMagnetics (TDEM) is suggested over the entire Argencourt fault zone, extending all ground survey lines by 1000 m to either side of the zone. This will result in a grid with the long axis oriented northwest and the survey lines oriented northeast-southwest with a nominal line length of 4 km. The zone is prospective for gold and base metals.

Additional staking is recommended along the trend of the Argencourt fault zone to the northwest and to the southeast of the current block given that the Uranium anomalies detected at this time are of higher value. The Uranium anomalies in the Howse lithotectonic zone suggest that additional targets can be developed to the northeast of the current claim group. Consideration should be given to expanding the claim block along this edge by a minimum of 1 km if possible.

8.5.2 Block II – Lac Mistamisk

8.5.2.1 Geology

Situated to the southeast of Block I and on the trend of the Argencourt fault zone, Block II includes the boundary between the lithotectonic Howse and Schefferville Zones. The fault zone exhibits dextral movement in the vicinity of the Cutus Lake North Showing # 176.

The Cutus Lake North Showing #176 is characterised by vein mineralisation within broad shear zones of the Argencourt fault zone. The host rock is a dolomite, probably of the Howse lithotectonic zone. Mineralisation consists of copper, silver, uranium oxide, chalcopyrite and quartz filling tension veins in the dolomite.

The Cutus Lake South Showing #175 is also dolomite hosted, but in this case the dolomite is in contact with a gabbro. Grab samples indicate the presence of copper, gold and silver.

The Otel Showing #182 is located on the shore of Otelnuk Lake. Massive pitchblende has been identified as has copper mineralisation. It is not uncommon to have coincident copper and uranium mineralisation. The mineralisation has been linked to the shear zones of the Argencourt thrust fault and associated cataclastic and fracture zones.

8.5.2.2 Gravity

The CBA map is dominated by a 10 milliGal gradient from a gravity high situated along the northeast edge of the survey block and dropping to a gravity low in the southwest corner of the block. The gravity high is faulted by a northwest – southeast trending dextral fault, possibly the Argencourt or related fault. The first vertical derivative (1VD) of the CBA is dominated by what appears to be a fault controlled north-westerly trending dense body of approximately 2700 metre length and 1000 metre width. The body is deep, Euler deconvolution depth estimates from the gravity data indicating a depth of approximately 1000 metres. There is an indication of a similar body to the north of the dextral fault along the eastern edge of the survey block.

8.5.2.3 Magnetics

The magnetic data is dominated by a major north-south trend and a minor north-northwest trend. The TMI products exhibit a significant amount of high frequency content suggesting very shallow or at surface magnetic sources. The dominant northwest trending fault with dextral movement is supported by the TMI. Shallow magnetic sources are also indicated by the lack of deep Euler depth solutions and a similar lack of deep solutions from the Source Parameter Imaging (SPI) processes. The deepest (~400 metres deep) solutions are consistent with the longer wavelength magnetic feature along the northern edge of the survey block.

The results of the calculated total horizontal derivative suggest that there are several shallow circular magnetic intrusives along the central north-northwest magnetic trend. This trend is coincident to the gravity 1VD body, but the resulting depths are significantly shallower than those indicated by the gravity data.

8.5.2.4 Radiometrics

There are two trends visible in the radiometric data: a north-south trend along the eastern margin of the survey block and a northwest trend in the southwest of the survey block. The north-south trend appears to be comprised predominately of Thorium whereas the northwest trend is composed predominately of Potassium. The Uranium response is unremarkable in that few coherent trends are visible, with Uranium "hotspots" appearing in a random fashion across the survey block.

8.5.2.5 Discussion of Results

There are essentially two (2) clusters of eleven (11) uranium anomalies in total within the survey block. The clusters are separated by the interpreted dextral fault and are referred to as the North Cluster and the South Cluster.

The North Cluster is comprised of five (5) uranium responses (Detail Area BII-A; U13 through U17) and is coincident with a gravity low and a magnetic high. This type of geophysical relationship would be consistent with a granitic body at depth. Euler depth solutions for both the magnetic and gravity solutions suggest a depth to source in this area of approximately 300 metres. The gravity and magnetic bodies are, in general, coincident in location and appear to be fault bounded and controlled. The majority of the uranium anomalies (U13, U14, U16, and U17) are distributed along

faults that define the shape and extent of the deep seated coincident gravity and magnetic body. The central uranium anomaly (U15) of the cluster is associated with a potential vertical pipe-like magnetic anomaly (M8) which is in the near surface. This cluster is to the north of Cutus Lake North Showing #176. The showing itself is on an interpreted magnetic fault bounding the magnetic high and is consistent with the observation of the showing occurring in a shear zone environment. The proximity of the uranium occurrences to the interpreted faults and showing suggests that the source may be consistent by vein mineralisation within the shear zones. The target zone is open to the north.

The second or South Cluster is located immediately to the south of the dextral fault and correlates to a residual gravity high (increased density contrast) and increased, although higher frequency, magnetic activity. The South Cluster (Detail Area BII-B) is comprised of four (4) uranium anomalies (U18 to U21), four (4) magnetic pipe-like intrusive features (M9 to M12) and the Cutus Lake South Showing. The northeast and southwest boundaries of the positive gravity and magnetic response appear to be fault controlled. The southwest boundary is also coincident with an interpreted magnetic dyke that based on the Euler depth solutions, should be visible at surface. The Cutus Lake South Showing #175 is within the interpreted bounds of the magnetic body. The geophysical response is consistent with the mapped geology of the showing, namely that a dolomite host is in contact with a gabbroic body. In the vicinity of Showing #175, the magnetic dyke to the southwest is very probably the gabbroic body referred to in the showing description. The pipe-like intrusives may be shallow off-shoots from a deeper mafic body.

Detail Area BII-C is located on the northeast shore of Otelnuk Lake and includes a shallow magnetic complex (M13) and uranium anomaly (U22) in addition to the Otel Showing #182. The associated magnetic body could be the cataclastic gabbro referred to in the showing description. The uranium anomaly is on the margin of the magnetic body and in close proximity to the showing.

Detail Area BII-D is on an extension of the gravity and magnetic high that is included in Detail Area BII-B. The uranium anomaly (U23) is at the junction of a north-south and a northeast-southwest fault and at the contact of the gravity/magnetic body with the host rock. It is anticipated that the geologic setting of this uranium anomaly will be similar to Cutus Lake South Showing, namely hosted in dolomite in contact with gabbro.

Detail Area BII-E is composed of two (2) pipe-like magnetic intrusives (M14 and M15) that should be exposed at surface anomalies are located within a triangle formed by faults interpreted from the magnetic data as trending east-west to the north of the targets; north-northwest to the west of the targets; and a northeast trending gravity to the east of the targets. The target area is to the south of the interpreted gabbro thought to underlie Detail Area BII-B and may be outliers of the same.

An isolated pipe-like magnetic target (M16) has been identified along the eastern margin of the survey block at 550550E, 6237200N. The target is located adjacent to a minor northeast trending fault and to the north of the major dextral fault. At this time ground follow-up has not been recommended, as the target is only partially covered by the airborne survey and therefore not properly or completely characterised.

8.5.2.6 Recommendations

A total of eleven (11) uranium and ten (10) magnetic anomalies of interest have been identified in Survey Block II. The anomalies have been grouped into five (5) areas for further study, labelled BII-A to BII-E. The mineralisation, based on the documented showings, differs if one is to the north of the dextral fault. The mineralisation in the north occurs in tensional stress fractures in the dolomite host filled by veins of quartz carrying copper silver, uranium and chalcopyrite. The mineralisation south of the fault tends to be shear zone related along the contact between dolomite and gabbro.

It is apparent from the geophysical surveys that the mineralisation is significantly more pervasive than indicated from the showing reports. Therefore detailed geologic mapping and sampling of all Detail Areas is high priority with the specific aim of further delineating the areal extent of the mineralisation within the shear zones and along the contact zones between the dolomite and the gabbro.

Of the five (5) Detail Areas, BII-A and BII-B are designated high priority; BII-C and BII-D are moderate priority and BII-E is currently low priority.

Table 25: Detail Area corner coordinates, Block II

Detail Area	UTM Easting	UTM Northing
BII-A	548660	6238863
	550485	6237789
	550485	6237789
	548660	6238863

Detail Area	UTM Easting	UTM Northing
BII-B	548024	6236055
	548528	6236047
	548545	6236815
	549263	6236815
	550072	6235956
	550080	6235221
	548974	6235172
	548867	6235576
	548049	6235585
	548024	6236055

Detail Area	UTM Easting	UTM Northing
BII-C	548123	6235064
	549271	6235064
	549271	6234057
	548123	6234057

Detail Area	UTM Easting	UTM Northing
BII-D	549981	6234858
	550485	6234858
	550485	6234305
	549981	6234305

Detail Area	UTM Easting	UTM Northing
BII-E	549227	6233870
	549847	6233870
	549847	6233187
	549227	6233187

All Detail Areas should include heavy mineral sampling for kimberlite indicator mineral identification. Geochemical sampling of the residual soils and lake sediment sampling for Uranium enrichment accompanied by detailed geologic mapping is required to effectively tie in the reported showings and the current geophysical survey data.

In Detail Area BII-A, surveying the area using the IP method may provide insight into the extent of the vein mineralisation. The remaining detail areas should be surveyed with a minimum of in loop TDEM to better determine the extent of the mineralisation present.

Additional staking is recommended in the following places:

1. Along the north edge of the survey block (extend Detail Area BII-A northwards) for a minimum of 1 km.
2. Extend the claims from Survey Block II to Survey Block I along the trend of the Argencourt fault.

8.5.3 Block III – Lac Drumlin

8.5.3.1 Geology

Survey Block III is the most northerly of the survey blocks. The block is located at the very edge of the Labrador Trough, composed of the Berard lithotectonic zone and Archaean basement crystalline rocks. As a result, the geology of the survey block is complex and punctuated by faulting and/or folding of the members of the Berard lithotectonic zone.

The survey block is centred on the Caribou Showing #234. This is arguably the most studied uranium occurrence of those covered by the current claims. The occurrence is hosted in Archaean granitic syentic rocks in pegmatite veins within the shear zones. The surface contact with the Labrador Trough Berard lithotectonic zone is approximately 500 metres to the south of the showing. The Labrador Trough rocks have been described as flat lying, unaltered and undisturbed

sedimentary sequences of the Ferriman Group. The current exposure of Archaean rocks is due to the erosion of the overlying Ferriman Group. Uranium with minor amounts of copper and gold disseminated in the shear zone is the dominant mineralisation.

8.5.3.2 Gravity

The CBA gravity is dominated by a very strong gradient extending from the northwest corner of the survey area extending initially south approximately midway through the survey block, then trending to the southeast corner. This trend is interpreted as a deep basement response (> 500 metres from Euler depth solutions) and is not expected to be visible on surface. Higher order derivative processing of the CBA further develops this trend into two (2) major fault systems, one trending north-south, and the other trending west-northwest.

A separate gravity anomaly trending north-northeast (azimuth 040) to the east of the Caribou Showing has a minimum strike length of 1000 metres and an approximate width of 200 metres. This discrete gravity body is interpreted as a possible extension of the Archaean granite-syenite which hosts the mineralised pegmatitic vein system of interest. Euler deconvolution depth estimates suggest that the source of the gravity anomaly averages a depth to source of 100 to 150 metres.

8.5.3.3 Magnetics

The dominant feature of the magnetic data is an interpreted syncline plunging to the south-southeast with the nose of the syncline immediately to the south of the Caribou Showing. This synclinal structure is interpreted as the Ferriman Group sedimentary cover that overlies the Archaean granite-syenite to the south of the Caribou showing. The magnetic survey may be responding to edges of an eroded, flat-lying horizontal sequence of layered strata containing sequences of magnetite enriched or mag-hematite enriched members. The syncline is open to the south.

The Caribous Showing is coincident with the edge of a magnetic body exhibiting a low or non-magnetic signature. This may represent an alteration zone where the destruction or remobilisation of magnetite has occurred, possibly related to the emplacement of the pegmatitic vein system.

North of the Caribou Showing, a well defined, east-west trending magnetic low. The low is terminated by a northeast trending magnetic high. Adjacent to this northeast trending magnetic high is a relative magnetic low, partially corresponding to the observed gravity high, suggesting that the geology in this location may be granitic.

In the northwest of the survey block, a strong northwest trend is observed.

8.5.3.4 Radiometrics

The Caribou Showing, if plotted in the correct location, is 500 metres to the northwest of the strongest uranium response (U24, > 11 ppm eU) recorded for the entire survey. The uranium anomaly exhibits a strike of approximately 040N for a length of approximately 400 metres. A second, larger, high amplitude uranium anomaly (U25) on trend with U24, exhibits a strike length of approximately 650 metres.

The potassium response in this survey block is anomalous in that there appears to be a general depletion of potassium in the vicinity of the Caribou Showing and anomaly U24, surrounded by a concentric ring of high potassium. A similar response is observed with anomaly U25. Migration of potassium in this manner suggests hydrothermal reworking of the host rock resulting in the mobility/displacement of potassium. This depletion zone may indicate the trend of the granite syenite hosting the uranium occurrences. The edges of the potassium depletion zone may also be prospective for gold.

8.5.3.5 Discussion of Results

Survey Block III is the most geologically and geophysically complex area covered by the current surveys. The Block is located on the cusp of the Labrador Trough and is majorly in Archaean granite-syenite terrane. The Ferriman Group of the Barard lithotectonic zone of the Labrador Trough is present to the south of the Caribou Anomaly and has been interpreted as a plunging syncline to the south. The radiometric survey has indicated a strong northeast trend which corresponds to a discrete gravity high and upon which the identified uranium targets are located. This trend is possibly overlain by the Ferriman sediments. The two (2) uranium anomalies identified exhibit the highest responses recorded during the survey.

Several small discrete magnetic anomalies (M17 to M21) that exhibit a pipe-like magnetic response have been observed almost exclusively in the Archaean granite terrane. These anomalous targets are associated with the northwest-southeast trend series of faulting.

8.5.3.6 Recommendations

Detailed geologic mapping is required to determine the relationship between the Caribou Showing and the Ferriman Group rocks in conjunction to the pronounced and rapid change in geomagnetic activity in the vicinity. The entire survey block is to be treated as a single detail area for follow-up surveying.

Geologic and geochemical sampling should be completed with the assays tailored not only for uranium, but also for gold. The trend extending across the survey area and connecting U25 to U24 to M20 is of the highest interest as additional uranium mineralisation may be present under the Ferriman Group cover rocks and along the pegmatite vein system.

If ground geological mapping and sampling confirms the presence of uranium in the vicinity of anomaly U25, then consideration should be given to expanding the existing gravity and airborne magnetic and radiometric coverage to the south and west of the current block.

Recommended geophysical exploration methods would be a detailed ground magnetic survey coupled with IP or TDEM surveying, focussed on the trend defined by anomalies U24 and U25.

Additional staking should be considered to the southwest, south, and northeast of the current block.

8.5.4 Block IV – Lac Wawiyusi Anatwayach

8.5.4.1 Geology

Survey Block IV is located at the extreme west end of the Labrador Trough. The survey area straddles the Lac Gerzine Outlier which has been classified as part of the Cambrian lithotectonic zone.

The general geology is thought to be composed of the Chakonipau conglomerates and arkosic sandstones.

The M.E.R.Q. has record of two (2) mineral occurrences (#164 and #165) that appear to be composed predominately of uranium mineralisation in boulder trains.

8.5.4.2 Gravity

The CBA map exhibits a weak gradient trending northeast from a high in the south to a low in the northeast. The bed of the riviere Giraud which crosscuts the north half of the survey area is coincident to a gravity low trending north-northwest and includes the boulder occurrence #164.

The 1VD of the CBA and other gravity derivative products suggest a sequence of dense, less dense, dense, les dense, dense east-west stratification of the rocks in the survey area. The interpreted fault zones that suggest a type of "horst and grabben" type tectonic environment appear to be buried under the cover rock, with Euler depths suggesting the faults run from near surface (<50 metres) to great depth (> 800 metres). It is possible that these faults extend into the Precambrian basement.

Boulder occurrence #165 is on a local gravity high which is trending east west for approximately 1 km.

8.5.4.3 Magnetics

The magnetic data mimics the gravity data to a high degree. The TMI map exhibits a similar trend to that observed in the gravity CBA data, namely the gradient varying from a magnetic high along the south edge of the survey block, to a low in the vicinity of the riviere Giraud, and rising to a high in the north.

The higher order processing of the magnetic data suggests a shallow overprint on a deep basement. The derivative maps are dominated by northeast – southwest and northwest – southeast trending faults. Evaluation of the Euler depth solutions strongly suggests two distinct populations of solutions; those are deep and related to regional trend, and a shallower series related to the northwest and northeast trend of the derivative maps.

Unlike the other survey areas, there are no pipe-like targets that can be identified from the magnetic data in this situation.

8.5.4.4 Radiometrics

The radiometric data in general exhibits a strong northeast trend, with some coincidence with the interpreted magnetic trend in this direction. There is correlation (weak) with the magnetic faults. The radiometric channels are indicating the last ice movement direction during the retreat of the glaciers during the ice age, and the current composition of the glacial overburden.

There is pronounced banding in the potassium and thorium maps, with both elements exhibiting the same trend of high-low concentrations trending northeast. The uranium response is uniformly mottled, with no preferred trend readily visible. There are however several possible uranium boulder responses identified. The boulder responses are labelled on the interpretation map as UB1 to UB7. There is excellent correlation with boulder anomaly UB7 and boulder occurrence #165.

The boulder responses do not appear to follow the general radiometric trend, but rather the deep seated east-west trend (as in the case of UB4, UB5 and UB6) or the northwest trend of the shallow magnetic responses as in the case of UB1, UB2 and UB3.

The ternary plot of the radioelements indicates that potassium and thorium occurs in the floodplain of the riveire Giraud and associated small lakes. The floodplain and the lakes exhibit a uranium response. A broad thorium and potassium high is observed trending northeast from 6228500N on the western edge of the survey block to 6233000N on the eastern edge. The trend is broken only where the riviere Giraud crosses the trend.

8.5.4.5 Discussion of Results

The geophysical and geological setting of survey Block IV suggests a complex evolution. The gravity east-west trend appears to be related to the broad large scale regional geology at depth below surface of 500^{+} metres. The central east-west high low gravity couplet has been interpreted as the Lac Grenier Outlier.

The magnetic derivative products suggest shallow trending northwest-southeast strata overlying the basement east-west trend. This in turn is overlain by glacial detritus and overburden which has been preferentially sorted and oriented in the direction of the last ice movement, in this instance, trending northeast.

A total of seven (7) boulder responses have been identified, and labelled, a brief summary is as follows:

Table 26: Potential Uranium enriched boulder responses, Block IV

Anomaly ID	UTM Easting	UTM Northing	Comments
UB1	441642	6234260	No magnetic signature; potentially in drainage, near contact between gravity units.
UB2	442015	6233223	May be associated with boulder occurrence 164; situated on a magnetic fault trending northeast.
UB3	443076	6232232	Potentially in the Riviere Gernier; near conjunction of northeast and east-west trending faults; near interpreted contact with Archaean and Lac Gerzine Outlier.
UB4	443146	6231265	At junction of magnetic faults; near gravity contact; hosted in the Lac Gerzine Outlier.
UB5	442773	3623111	On same northeast trending fault as UB4; near northwest trending fault; in gravity low. Hosted in the Lac Gerzine Outlier.
UB6	442167	6231135	Just off of fault and trend defined by UB4 & UB5; in gravity low. Hosted in the Lac Gerzine Outlier.
UB7	442481	2630239	Coincident with boulder occurrence #165; on northwest trending fault and in close proximity to magnetic and gravity contact to north. Potentially hosted in the Archaean.

8.5.4.6 Recommendations

It is recommended that all potential boulder responses be verified on the ground through geologic mapping and sampling. The use of a hand held spectrometer or Geiger counter is recommended. Additionally, confirmation of the ice retreat direction and extent of glacial overburden (if present) is required. Upon completion of this phase, the geophysics can be re-evaluated and an exploration plan determined.

Any boulder occurrences that are confirmed should be followed out using till and geochemical sampling methods and boulder sampling until the source can be determined.

8.5.5 Block V - Lac Wawiyusi Anatwayach

8.5.5.1 Geology

Survey Block IV is located at the extreme southwest end of the Labrador Trough in the Lac Pons area. The survey area straddles a small outlier to the south of the Lac Gerzine Outlier. The outlier has been classified as part of the Cambrian lithotectonic zone.

The general geology is thought to be composed of the Chakonipau conglomerates and arkosic sandstones surrounded by felsic intrusives.

The M.E.R.Q. has record of one (1) mineral occurrence (#166) that appears to be composed predominately of uranium mineralisation in boulder trains.

8.5.5.2 Gravity

The Bouguer gravity (CBA) map indicates a ">" shaped density contact that dominates the survey block. The gravity high which is on the outside edge of the ">" is though to indicate the felsic volcanics and granites that surround the Outlier. The inside of the ">" is a gravity low, consistent with a thickening sedimentary section to the west.

Application of derivative processing and Source Edge Detection (SED) further refines the ">" by separating the survey block into three (3) gravity units: a dense gravity unit to the north; a central gravity low trending east-northeast; and a south dense gravity unit. The central low is cut by a narrow north-northwest trending dense gravity arch which may be attributed to a mafic dyke or similar feature.

Euler deconvolution solutions for the CBA suggest that the gravity faults extend to surface from depth.

8.5.5.3 Magnetics

The TMI maps and associated products exhibit a similar pattern to the gravity. The north and south margins of the survey area are magnetic and correlate to gravity highs in the same locations. Dominant trends are east-northeast for the deep seated north and south magnetic bodies. There is a slightly elevated magnetic background in the vicinity of the northwest gravity arch running through the centre of the of the survey block.

The derivative maps suggest that the metasedimentary sequence may be similar to that encountered in Block III. It can be inferred from the magnetic derivative maps that there may be a west plunging synclinal feature composed of the conglomerates and sandstones of the Outlier. The implication is that the metasedimentary section becomes thicker and deeper to the west, under Lac Pons.

8.5.5.4 Radiometrics

The Total Count, Potassium and thorium radiometric maps all exhibit the ">" shape anomaly and correlate in this respect to the magnetic and gravity data. However, much of this correlation is the result of the effect of the Lac Pons and associated lakes on the spectrometer data. The lakes must be deeper than 2 or 3 metres as the radiometric counts decrease to background levels of zero (0), indicative of a column water deeper than 1 metre and therefore masking any gamma ray radiation from detection.

Uranium count rates are generally low with the exception of in the vicinity of the boulder occurrence #166 and immediately to the east of this occurrence along an interpreted magnetic fault (anomalies U26 and U27).

8.5.5.5 Discussion of Results

The survey block can be divided into three basic units:

1. A magnetic mass at the north end with a coincident gravity anomaly;
2. A central, possibly sedimentary unit, with coincident low gravity and magnetic signatures; and
3. A southern mass characterised by a very strong gravity signature with coincident strong magnetic signature.

Bridging the two extremes is a well defined, narrow, north-south trending gravity "dyke" that is offset by nominally east-west faulting. Euler deconvolution analysis suggests that all faulting is near vertical in aspect.

Two (2) well defined uranium anomalies (U26 and U27) are present in the central portion of the survey block. Anomaly U26 is coincident with boulder occurrence #166 and occurs along a magnetic and gravimetric fault that suggests a relative sinstral movement. Anomaly U26 is also coincident with the interpreted gravity "dyke".

As the metasedimentary unit hosting the uranium anomalies is thought to consist of conglomerate and sandstone units, the central portion of the survey block is ideal for hosting a uranium deposit and therefore very prospective.

There is a poorly defined trend in the magnetic derivative products that suggests that the metasediments are plunging to the west from the gravity "dyke" intersection.

8.5.5.6 Recommendations

Given that the geology and geophysics appear to presenting favourable coincident responses for uranium mineralisation, follow-up work on the entire Block V survey area should be assigned high priority.

The second anomaly U27 should be located and verified on the ground. Extensive detailed geologic mapping of the metasedimentary unit and investigation of the gravity "dyke", particularly in the Anomaly U26, occurrence #166 area is required. When confirmation of a sedimentary host rock is complete, delineation of the horizon can be planned for surveying by ground TDEM survey.

If the mineralisation can be confirmed along the east-west fault zone, then additional claims should be staked to completely cover the outlier.

8.6 Summary

The recently completed multiple discipline geophysical surveys over Blocks I, II, III, IV and V in the Labrador Trough of Northern Quebec for Waseco Resources Inc. has identified fifty-five (55) targets for additional study and potentially drilling. The anomalies may be broken down as follows:

- 27 Uranium anomalies (25 High Priority; 2 Moderate Priority)
- 21 magnetic anomalies (17 High Priority, 1 Moderate Priority, 3 Low Priority)
- 7 Uranium boulder anomalies (All Low Priority)

The follow-up studies over the majority of the anomalies require the completion of detailed geologic mapping and ground confirmation of the anomaly presence prior to the spotting of diamond drill test hole collars. The ground follow-up should incorporate some or all of the following methodologies:

- Geologic mapping including prospecting using a Geiger counter or hand held spectrometer and grab sampling,
- Heavy mineral sampling for kimberlite indicator minerals where appropriate,
- Geochemical sampling, including stream sediment and lake sediment sampling where appropriate for copper, gold and silver in addition to uranium,
- Till sampling in areas where glacial overburden coverage is a problem,
- Ground magnetometer surveying to confirm the location of the magnetic targets,
- Ground spectrometer surveying to be used to calibrate and confirm the airborne radiometric survey.
- Detailed surveying for conductive sulphide deposits at depth using either IP or TDEM where appropriate.

The following table provides a summary of the anomalies with respect to the priority and type of work required to further prove up the target in preparation for diamond drilling:

Table 27: Anomaly Summary Table

Survey Block	Anomaly	UTM Easting	UTM Northing	Methods to use	Priority
I	U1	537233	6250022	Geological Mapping, Geochemical Sampling, Heavy Mineral Sampling, IP/TDEM, Mag/Spec Survey	High
	U2	537747	6247965		
	U3	539492	6248557		
	U4	540614	6249414		
	U5	538822	6247358		
	U6	539741	6247311		
	U7	540349	6247342		
	U8	541455	6248261		
	U9	537327	6245924		
	U10	541330	6246345		
	U11	542624	6245363		
	U12	539975	6243743		
	M1	540333	6249461		
	M2	541424	6247887		
	M3	538775	6246469		
	M4	538931	6246220		

	M5	539290	6245737		
	M6	540240	6244647		
	M7	540598	6244725		
II	U13	548938	6238795	*Detail Area BII-A* Geological Mapping, Geochemical Sampling, Heavy Mineral Sampling, IP/Mag/Spec Survey	High
	U14	549067	6238277		
	U15	549420	6238289		
	U16	550232	6238712		
	U17	550091	6238253		
	M8	549314	6238053		
	U18	548938	6236547	*Detail Area BII-B* Geological Mapping, Geochemical Sampling, Heavy Mineral Sampling, TDEM/Mag/Spec Survey	High
	U19	549196	6236088		
	U20	549891	6235805		
	U21	548090	6236017		
	M9	549008	6236429.		
	M10	549232	6235735		
	M11	549408	6235723		
	M12	549479	6235382		
	U22	548985	6234793	*Detail Area BII-C* Geological Mapping, Geochemical Sampling, Heavy Mineral Sampling, TDEM/Mag/Spec Survey	Moderate
	M13	548726	6234440		
	U23	550232	6234581	*Detail Area BII-D* Geological Mapping, Geochemical Sampling, Heavy Mineral Sampling, TDEM/Mag/Spec Survey	Moderate
	M14	549420	6233687	*Detail Area BII-E* Geological Mapping, Geochemical Sampling, Heavy Mineral Sampling, TDEM/Mag/Spec Survey	Low
	M15	549597	6233510		
	M16	550538	6237147	None at this time	Low
III	U24	453420	6336135	Geological Mapping, Geochemical Sampling, Heavy Mineral Sampling, IP/TDEM, Mag/Spec Survey	High
	U25	452304	6334811		
	M17	452738	6337203		
	M18	452572	6336989		
	M19	451759	6335645		
	M20	454392	6337120		
	M21	453840	6335294		
IV	UB1	441642	6234260	Geological Mapping, Geochemical Sampling Mag/Spec Survey	Low
	UB2	442015	6233223		
	UB3	443076	6232232		
	UB4	443146	6231265		
	UB5	442773	3623111		

	UB6	442167	6231135		
	UB7	442481	2630239		
V	U26	442724	6208303	Geological Mapping, Geochemical Sampling, Heavy Mineral Sampling, TDEM/Mag/Spec Survey	High
	U27	443501	6208143		

It has also been recommended that additional claims be staked to include the extension of promising geophysical anomaly trends outside of the current claim block boundaries. The following table summarises these recommendations:

Table 28: Additional Claim Staking Summary Table

Survey Block	Stake Additional Claims
I	Stake to the northwest and southeast along geologic contact. Stake along northeast for distance of 1 km minimum from existing claims.
II	Stake along north edge of survey block for minimum of 1 km above existing claims. Stake entire gap between Block I and Block II.
III	Stake claims along southwest, and south of survey block for minimum of 1 km around existing claims, Stake claims along northeast for minimum of 1 km above existing claims.
IV	No additional staking at this time.
V	Stake remainder of Outlier to the west.

9. DELIVERABLE PRODUCTS

The survey data are presented as colour/contour maps on paper, produced at a scale of 1:20,000. A set of report-sized colour/contour images, on paper, is included as Appendix 6. The basic co-ordinate system used is NAD83, Universal Transverse Mercator Zone 19N. All digital data are also presented on CD-ROM in ASCII format.

The deliverable items of this survey are:

9.1 Maps

The following maps, produced for each Survey Block, at a scale of 1:20,000, are delivered in five (5) paper copies.

- Gravity Station Location
- Digital Terrain Model from GPS Survey
- Free Air Anomaly
- Bouguer Anomaly (for Bouguer densities of 2.45 g/cm^3, 2.67 g/cm^3 and 2.80 g/cm^3)
- Terrain Corrections
- Complete Bouguer Anomaly (CBA)
- Calculated First Vertical Derivative Map (1VD) of the CBA
- Analytic Signal of the CBA
- Total Horizontal Derivative of the CBA
- Gravity Euler Deconvolution Depth Solutions (for S.I. = 0, 1)
- Flight Path with Planimetry
- Total Magnetic Intensity (TMI)
- Reduction to the Magnetic Pole (RTP) of the TMI
- Calculated First Vertical Derivative (1VD) of the RTP-TMI
- Calculated Second Vertical Derivative (2VD) of the RTP-TMI
- Analytic Signal of the TMI
- Calculated Total Horizontal Derivative of the RTP-TMI
- Magnetic Euler Deconvolution Depth Solutions (for S.I. = 1, 2)
- Source Parameter Imaging (SPI)
- Total Count
- Uranium
- Thorium
- Potassium
- Uranium / Thorium (U/Th) Ratio
- Uranium / Potassium (U/K) Ratio
- Potassium / Thorium (K/Th) Ratio
- Ternary Plot
- Source Edge Detection (SED)
- Geophysical Interpretation

9.2 Digital Data

The edited field and processed digital data are delivered in five (5) copies, in ASCII code, on CD-ROM. The final processed line and grid data, in GEOSOFT format, are also delivered in two (5) copies on CD-ROM. Full descriptions of the digital data formats are included in this final report (see below) and as text files on each CD-ROM. Each CD-ROM has a README.TXT file describing the contents and the file formats.

9.3 Report

Five (5) copies of a survey report were delivered, complete with all final maps as page size maps. This report provides information about the acquisition, processing and presentation of the survey data. The report was a collaborative effort on the part of Dr. Tomas Grand, Mr. John Irvine, and Mr. Robert Hearst.

Respectfully submitted,
McPhar Geosurveys Ltd.

Robert Hearst, M.Sc., P.Geoph. (NAPEG)
General Manager - Operations